HHS Public Access

Author manuscript

Cell. Author manuscript; available in PMC 2018 November 02.

Published in final edited form as:

Cell. 2017 November 02; 171(4): 918–933.e20. doi:10.1016/j.cell.2017.09.040.

Assembly and Function of Heterotypic Ubiquitin Chains in Cell Cycle and Protein Quality Control

Richard G. Yau[1,2], **Kerstin Doerner**[1], **Erick R. Castellanos**[3], **Diane L. Haakonsen**[1,2], **Achim Werner**[1], **Nan Wang**[6,7], **X. William Yang**[6,7], **Nadia Martinez-Martin**[5], **Marissa L. Matsumoto**[3,*], **Vishva M. Dixit**[4,*], and **Michael Rape**[1,2,8,*]

[1]University of California at Berkeley, Department of Molecular and Cell Biology, Berkeley, CA 94720

[2]Howard Hughes Medical Institute, Berkeley, CA 94720

[3]Genentech Inc., Department of Structural Biology, South San Francisco, CA 94080

[4]Genentech Inc., Department of Physiological Chemistry, South San Francisco, CA 94080

[5]Genentech Inc., Department of Microchemistry, Proteomics, and Lipidomics, South San Francisco, CA 94080

[6]Center for Neurobehavioral Genetics, Semel Institute for Neuroscience & Human Behavior, University of California, Los Angeles, Los Angeles, California, USA

[7]Department of Psychiatry and Biobehavioral Sciences, David Geffen School of Medicine at UCLA, University of California, Los Angeles, Los Angeles, California, USA

Summary

Posttranslational modification with ubiquitin chains controls cell fate in all eukaryotes. Depending on the connectivity between subunits, different ubiquitin chain types trigger distinct outputs, as seen with K48- and K63-linked conjugates that drive protein degradation or complex assembly, respectively. Recent biochemical analyses also suggested roles for mixed or branched ubiquitin chains, yet without a method to monitor endogenous conjugates, the physiological significance of heterotypic polymers remained poorly understood. Here, we engineered a bispecific antibody to detect K11/K48-linked chains and identified mitotic regulators, misfolded nascent polypeptides, and pathological Huntingtin variants as their endogenous substrates. We show that K11/K48-linked chains are synthesized and processed by essential ubiquitin ligases and effectors that are mutated across neurodegenerative diseases; accordingly, these conjugates promote rapid proteasomal clearance of aggregation- prone proteins. By revealing key roles of K11/K48-linked chains in cell cycle and quality control, we establish heterotypic ubiquitin conjugates as important carriers of biological information.

*to whom correspondence should be addressed: mrape@berkeley.edu; dixit.vishva@gene.com; matsumoto.marissa@gene.com.
8lead author

Graphical abstract

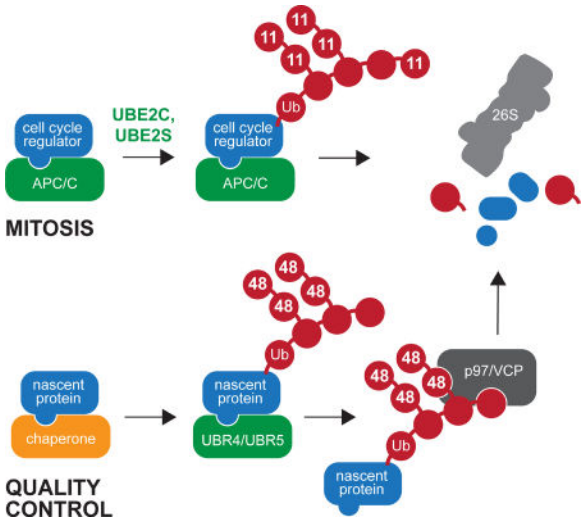

Keywords

ubiquitin; ubiquitin chain; branched ubiquitin chain; anaphase-promoting complex; protein quality control; proteasome

Introduction

Posttranslational modification with the highly conserved and essential protein ubiquitin controls cell division, differentiation, and survival in all eukaryotes (Harper and Bennett, 2016; Husnjak and Dikic, 2012; Ravid and Hochstrasser, 2008; Skaar et al., 2013; Yau and Rape, 2016). The precision and versatility of ubiquitylation in signal transduction depends on the ability of cells to assemble multiple conjugates with distinct topologies and functions. Attachment of a single ubiquitin, referred to as monoubiquitylation, typically alters a target's interaction landscape (Husnjak and Dikic, 2012). In addition, cells can assemble polymeric ubiquitin chains, in which subunits are connected through an isopeptide bond between eight possible attachments sites on one ubiquitin and the carboxy-terminus of the next. Homotypic chains are characterized by a single predominant linkage, as in K11- and K48-linked polymers that promote proteasomal degradation (Chau et al., 1989; Jin et al., 2008), or M1- and K63-linked conjugates that coordinate the reversible assembly of signaling complexes (Spence et al., 1995; Tokunaga et al., 2009; Wang et al., 2001). By contrast, heterotypic ubiquitin chains contain multiple linkages and adopt mixed or branched topology (Yau and Rape, 2016). The signature motifs of branched chains are ubiquitin molecules that are modified on two or more residues at the same time.

Linkage-specific antibodies and mass spectrometry provide powerful approaches to study homotypic ubiquitylation at the physiological level (Matsumoto et al., 2012; Matsumoto et al., 2010; Newton et al., 2008; Xu et al., 2009). By contrast, the analysis of heterotypic chain types has relied entirely on indirect means, such as *in vitro* reconstitution, treatment of purified chains with deubiquitylases, or expression of engineered ubiquitin variants. Such

experiments suggested that M1/K63-linked chains control NFκB transcription factor activation (Emmerich et al., 2016; Emmerich et al., 2013; Wertz et al., 2015), while K11/K48-branched chains signal the degradation of cell cycle regulators during mitosis (Meyer and Rape, 2014). Similar *in vitro* or protein engineering evidence exists for K48/K63-branched, K29/K48-linked or more complex heterotypic chains (Kim et al., 2007; Koegl et al., 1999; Kristariyanto et al., 2015; Liu et al., 2017; Ohtake et al., 2016). These findings implied that cells use heterotypic chains for signal transduction, yet without a method to monitor endogenous polymers *in vivo*, the abundance, function, and importance of mixed or branched ubiquitin chains remain very poorly understood.

Synthesis of ubiquitin chains requires the coordinated action of E1 activating enzymes, E2 conjugating enzymes, and E3 ligases (Komander and Rape, 2012). Most E3 ligases use dedicated domains to recruit specific substrates, while they determine the linkage specificity of chain formation dependent on their catalytic module: members of the HECT- or RBR-families of E3s, which contain an active site cysteine charged with ubiquitin, directly select the ubiquitin residue for chain elongation (Kamadurai et al., 2009; Kim and Huibregtse, 2009). By contrast, RING-E3s help transfer ubiquitin from the active site of an E2 to target lysine residues and rely on their E2s to establish chain topology (Plechanovova et al., 2012; Wickliffe et al., 2011). The human genome contains ~600 E3s, several of which are encoded by essential genes or mutated in tumorigenesis, neurodegeneration, and developmental diseases (Deshaies and Joazeiro, 2009; Lipkowitz and Weissman, 2011; Rotin and Kumar, 2009). However, even *in vitro* few E3 ligases are known to synthesize mixed or branched polymers, and mechanisms of heterotypic chain production are not understood. The impact of heterotypic chains on signal transduction is therefore not known, and many pathways that depend on these conjugates likely await discovery.

To address these issues, we developed a bispecific antibody that allowed us to identify mitotic regulators, misfolded nascent polypeptides, and pathological Huntingtin as physiological substrates of branched ubiquitin chains containing both K11- and K48-linkages. We found that K11/K48-branched polymers ensure rapid substrate delivery to the proteasome, which prevents accumulation of aggregation-prone nascent proteins. Our findings place K11/K48-linked chains at the heart of cell cycle and protein quality control, two essential pathways that rely on rapid and efficient protein degradation. Consistent with this notion, we show that enzymes and effectors of K11/K48-linked chains are encoded by essential genes and mutated across neurodegenerative diseases. Our work establishes that endogenous heterotypic ubiquitin chains play important roles in cellular signaling pathways.

Results

A K11/K48-bispecific antibody recognizes heterotypic ubiquitin chains

Starting with K11- and K48-monospecific antibodies (Matsumoto et al., 2010; Newton et al., 2008), we used knobs-into-holes heterodimerization technology (Merchant et al., 1998) to create a bispecific antibody, in which one arm recognizes the K11-ubiquitin linkage and the other binds the K48-linkage (Figure 1A; Figure S1A). As controls, we engineered K11/gD and K48/gD antibodies that pair a ubiquitin-directed antibody arm with one that detects an unrelated viral protein (Figure 1A). We purified these antibodies to homogeneity and

characterized them by SDS-PAGE, analytical size-exclusion chromatography, multi-angle light scattering, and mass spectrometry (Figure 1B; Figure S1B–D, S2A–C; Table S1, 2). This validation confirmed that we had engineered and purified well-behaved antibody species.

We used surface plasmon resonance (SPR) to assess the specificity of these antibodies towards K11/K48-branched ubiquitin trimers. At high densities of immobilized trimer (700 RUs), the K11/K48-bispecific antibody showed ~500–1,000-fold higher affinity for K11/K48-branched ubiquitin than K11/gD and K48/gD antibodies (Table S3, 4; Figure S1H). By contrast, K11/K11- or K48/K48-monospecific antibodies bound K11/K48-branched trimers with a similar affinity as the bispecific antibody, suggesting that they recognize their linkage independently of branching. At lower immobilization densities (150 RUs), the bispecific antibody displayed a slightly reduced affinity towards K11/K48-branched trimers, while the affinity of the control antibodies was unchanged. This indicated that the K11/K48-bispecific antibody acts as a coincidence detector that gains avidity from simultaneous detection of K11- and K48-linkages. In agreement with this notion, the K11/K48-bispecific antibody was able to detect a 1:1 mixture of immobilized K11- and K48-linked dimers, which mimics the proximity of these linkages in branched ubiquitin molecules, while it showed a similar low affinity to homotypic K11- or K48-linked dimers or tetramers as both control bispecific antibodies (Table S3, 4).

We next tested the ability of the K11/K48-bispecific antibody to detect branched ubiquitin conjugates in Western blot analyses. Notably, while the K11/K48-bispecific antibody efficiently recognized K11/K48-branched trimers, it failed to detect monomeric or dimeric ubiquitin, including K11- or K48-linked di-ubiquitin species (Figure 1C). This behavior was different from K11/K11- and K48/K48-monospecific antibodies, which bound ubiquitin dimers and trimers containing their cognate linkage, as well as from K11/gD and K48/gD control antibodies, which did not produce any signal under these conditions. The K11/K48-bispecific antibody displayed similar selectivity towards variants of branched ubiquitin: while it readily recognized K11/K48-branched trimers, it did not detect their K11/K63-, K48/K63-, or M1/K63- branched counterparts (Figure 1D, E). Using an engineered ligation system (Meyer and Rape, 2014), we found that the K11/K48-bispecific antibody recognized high molecular weight (MW) K11/K48-linked polymers in strong preference over homotypic K11- or K48-linked chains (Figure 1F). Moreover, we used radiolabeled substrates modified with high-MW K11/K48- branched chains to quantify antibody specificity under immunoprecipitation conditions. Similar to SPR and Western blot analyses, the K11/K48-bispecific antibody displayed a much higher affinity for K11/K48-branched chains than K11/gD or K48/gD control antibodies (Figure 1G).

The SPR analysis had indicated that the K11/K48-bispecific antibody might function as a coincidence detector that binds to both K11- and K48-linkages at the same time. Consistent with this notion, the K11/K48-bispecific antibody detected mixed trimers with proximal K11- and K48- linkages with similar efficiency as K11/K48-branched trimers (Figure S1E). However, the K11/K48-bispecific antibody did not recognize mixtures of separate K11- and K48-linked dimers in Western blot analyses, nor did it bind mixtures of K11- and K48-linked homotypic chains (Figure S1F, G). Thus, the striking avidity gain provided by

coincidence detection allows the bispecific antibody to selectively report on heterotypic K11/K48-linked chains, yet two important control experiments should be performed before conclusions about chain topology are drawn: first, as K11/gD and K48/gD antibodies have low, yet significant, affinity for their cognate linkages, both control antibodies must be implemented in Western blots or quantitative mass spectrometry at the same concentration and incubation time as the K11/K48-bispecific antibody. Second, as a coincidence detector detects proximal K11- and K48-linkages, biochemical experiments should be used to distinguish between neighboring homotypic chains on the same substrate, mixed chains, or branched ubiquitin conjugates. In the remainder of this study, we demonstrate how the unique binding properties of the K11/K48-bispecific antibody can be exploited to reveal the critical role of heterotypic ubiquitin chains in cellular signaling.

The APC/C assembles K11/K48-branched chains during mitosis

We first used the K11/K48-bispecific antibody to analyze the products of the anaphase-promoting complex (APC/C), an E3 that controls cell division in all eukaryotes. Previous work with ubiquitin mutants had indicated that the APC/C labels substrates with K11/K48-branched chains, but whether the APC/C produces such conjugates under physiological conditions remained unclear (Meyer and Rape, 2014). *In vitro*, the APC/C-dependent synthesis of branched chains is initiated by an E2 with broader linkage-specificity, such as UBE2C (Kirkpatrick et al., 2006), whereas branching is catalyzed by the K11- and APC/C-specific E2 UBE2S (Meyer and Rape, 2014). Consistent with these studies, the K11/K48-bispecific antibody showed that APC/C, UBE2C and UBE2S labeled their mitotic substrate cyclin A with K11/K48- linked chains (Figure 2A; Figure S3A). The APC/C-dependent production of heterotypic chains required equal concentrations of UBE2C and UBE2S, a condition that is specifically encountered during mitosis (Rape and Kirschner, 2004; Williamson et al., 2009). Similar observations were made using a different substrate, securin (Figure S3B), or a distinct initiating E2, UBE2D3 (Figure S3C).

To assess the ubiquitin chain topology assembled by the APC/C, we performed *in vitro* reactions with mixtures of ubiquitin^{K11R} and ubiquitin^{K48R} variants. Under these conditions, the APC/C could produce proximal homotypic chains or mixed polymers, but not branched conjugates, because no ubiquitin molecule contains both K11 and K48 (Meyer and Rape, 2014). Independently of substrate or initiating E2, the K11/K48-bispecific antibody only detected ubiquitin chains if the APC/C was incubated with wild-type ubiquitin, but not if reactions were carried out in the presence of both ubiquitin^{K11R} and ubiquitin^{K48R} (Figure S3A–C). These observations provide direct evidence for the APC/C synthesizing K11/K48-branched ubiquitin chains.

Supporting these *in vitro* results, we found in synchronization and microscopy experiments that K11/K48-linked chains increase in abundance during mitosis, when the APC/C ubiquitylates most of its targets (Figure 2B; Figure S3D, E). We did not detect K11/K48-linked chains in mitotic cells depleted of the APC/C-specific E2 UBE2S (Figure 2B; Figure S3E), which suggests that during cell division most K11/K48-linked polymers are attached to APC/C substrates. Proteomic analyses from mitotic cells reaffirmed the role of the APC/C in the synthesis of K11/K48-linked conjugates, as several substrates or regulators of the

APC/C were enriched in K11/K48-bispecific affinity-purifications compared to control K11/gD and K48/gD immunoprecipitations (Figure S3F). Candidate substrates included the APC/C co-activator CDC20 that was ubiquitylated at Lys490 (Figure 2C). Modification of CDC20 at this site was implicated in spindle checkpoint silencing, a reaction that *in vitro* is brought about by the APC/C, UBE2S, and branched ubiquitin chains (Alfieri et al., 2016; Meyer and Rape, 2014; Reddy et al., 2007; Williamson et al., 2009; Yamaguchi et al., 2016).

We confirmed modification of endogenous CDC20 and cyclin A by denaturing purification of K11/K48-branched chains from mitotic cells (Figure 2C). Using native affinity-purification, we also showed that endogenous NEK2A was decorated with such conjugates (Figure 2D). We detected increased K11/K48-specific modification of APC/C substrates if the proteasome was inhibited (Figure 2C, D), which is consistent with the proposed role of K11/K48-branched chains in protein degradation (Meyer and Rape, 2014). Together, these results validate the K11/K48-bispecific antibody *in vivo* and show, to our knowledge for the first time, that endogenous proteins are modified with heterotypic ubiquitin chains. During mitosis, K11/K48-linked conjugates contain multiple blocks of K11-linked chains (Meyer and Rape, 2014), are assembled by the APC/C, and likely function as proteasome-targeting signals.

K11/K48-linked chains label newly synthesized and aggregation-prone proteins

The discovery of K11/K48-branched chains relied on biochemical analyses of the APC/C (Meyer and Rape, 2014), an approach that cannot be used to reveal roles of heterotypic polymers that are assembled by unknown E3 ligases or act in uncharacterized signaling pathways. As an alternative strategy, we used our bispecific antibody to screen for conditions that show high levels of K11/K48-linked conjugates and hence might depend on their signaling function. We found that K11/K48-linked chains accumulated in cells experiencing proteotoxic stress caused by inhibition of the proteasome, HSP70, or HSP90 (Figure 3A). Several other conditions that elicit strong ubiquitylation responses, such as DNA damage, mitochondrial dysfunction, ER overload, or oxidative stress, did not cause a global increase in the abundance of K11/K48- linked chains. Affinity-purification of K11/K48-linked polymers showed a marked enrichment of K11- and high-MW K48-linkages, but not M1- or K63-linkages (Figure S4A). Together, these results suggested that proteotoxic stress promotes formation of high-MW heterotypic K11/K48- linked chains, which contribute significantly to the cellular ubiquitin pool.

To dissect the topology of the ubiquitin chains formed under proteotoxic stress, we purified K11/K48-linked conjugates from cells expressing TEV-cleavable ubiquitin. As described before (Liu et al., 2017; Meyer and Rape, 2014), treatment of conjugates containing ubiquitin- TEV with TEV protease results in a ~2kDa “stamp” per subunit attached to wild-type ubiquitin molecules. Branched chains are characterized by ubiquitin subunits that are modified on two or more lysine residues, and thus, display two or more stamps, whereas mixed chains or independent homotypic polymers produce only a single stamp. We found that cells efficiently synthesize K11/K48-branched chains upon proteotoxic stress (Figure 3B; Figure S4B). As expected from its mechanism of coincidence detection, the K11/K48-

bispecific antibody enriched branched ubiquitin chains more efficiently than a pan-ubiquitin antibody used for comparison (Figure S4B).

To characterize the formation of K11/K48-branched chains in cells, we made use of the observation that HSP70- or HSP90-inhibition leads to accumulation of misfolded, aggregation- prone proteins (Bennett et al., 2007; Ellis and Minton, 2006; Hipp et al., 2014). As aggregates are still recognized by the ubiquitylation, but not the degradation machinery, they can be investigated for ubiquitin marks attached to misfolded proteins *in vivo*. In agreement with our experiments in lysates, HSP70- and HSP90-inhibition triggered the formation of cytoplasmic aggregates that were extensively decorated with K11/K48-linked chains (Figure 3C; Figure S4C). We detected similar K11/K48-positive aggregates in 293T cells, untransformed human embryonic stem cells, neuronal precursors, and differentiated neurons (Figure S4C, D). These findings indicated that multiple cell types respond to the accumulation of aggregation-prone proteins with the production of K11/K48-branched chains.

A large fraction of HSP70 and HSP90 clients are newly synthesized proteins that fail to fold upon release from ribosomes (Balchin et al., 2016; Brandman and Hegde, 2016; Harper and Bennett, 2016). Proteins that have not reached their native conformation even after multiple attempts of chaperone-assisted folding are rapidly degraded by the ubiquitin-proteasome system (Wang et al., 2015a; Wang et al., 2013). Suggesting that K11/K48-specific quality control primarily targets such nascent polypeptides, inhibition of mRNA translation by cycloheximide, emetine, or harringtonine prevented the accumulation of K11/K48-linked conjugates (Figure 3D; Figure S4E–H), and no K11/K48-positive aggregates were detected under these conditions (Figure 3C; Figure S4C, D). By contrast, inhibition of transcription by α- amanitine had no effect (Figure 3C, D), and cycloheximide treatment did not ablate formation of K11/K48-linked chains during mitosis, when such conjugates label cell cycle regulators targeted by the APC/C (Figure S4I). To directly test for modification of newly synthesized proteins, we treated cells with puromycin, which is incorporated into nascent chains and releases misfolded proteins from ribosomes. Both denaturing and native affinity-purification of specific chain types revealed that puromycylated proteins were strongly labeled with K11/K48-linked conjugates (Figure 3E; Figure S4J), and puromycylated polypeptides were recruited to aggregates that were positive for K11/K48-linked chains (Figure 3F). From these collective results, we infer that cells modify newly synthesized and misfolded proteins with K11/K48-linked ubiquitin chains.

Identification of enzymes and effectors of K11/K48-specific quality control

Previous work had indicated that quality control networks direct up to 15% of newly synthesized proteins towards ubiquitin- and proteasome-dependent degradation (Wang et al., 2013), yet the E3 ligases or ubiquitin-binding proteins of this pathway have not been identified. Our discovery that nascent proteins are modified with K11/K48-branched chains offered an opportunity to discover components of this quality control network: we hypothesized that effectors, such as chaperones or proteasome shuttles, bind the ubiquitylated targets, while E3 ligases might modify themselves with the same K11/K48-linked conjugates that they transfer onto substrates.

We therefore used label-free quantitative mass spectrometry to isolate proteins that were enriched in K11/K48- compared to K11/gD- and K48/gD-control immunoprecipitations. To focus on quality control rather than cell division, we conducted these experiments in puromycin- treated, asynchronous cells with little or no APC/C activity. We found that HSP90 as well as the ribosome-associated chaperone BAG6 were enriched in K11/K48-specific affinity-purifications (Figure 4A). HSP70 was also abundant in these precipitations, yet due to high background binding, it was not enriched compared to the control reactions. In addition, we noted strong enrichment of the E3s UBR4, UBR5, and HUWE1 (Figure 4A), while we found no binding for the APC/C, which is mainly active during mitosis; Listerin or ZNF598, which modify proteins on stalled ribosomes (Bengtson and Joazeiro, 2010; Brandman et al., 2012; Juszkiewicz and Hegde, 2017; Shao et al., 2015; Sundaramoorthy et al., 2017); or CHIP, which can ubiquitylate HSP70 or HSP90 clients (Meacham et al., 2001; Younger et al., 2006). As effectors of K11/K48- linked chains, we identified the p97/VCP segregase and its receptors, including NSFL1/p47; proteasome shuttles, such those of the UBQLN family; low amounts of p62/SQSTM1, which had been implicated in proteasomal and autophagosomal delivery; and the 26S proteasome (Figure 4A). By contrast, we did not recover any E3 ligase, deubiquitylase, or effector with M1- or K63- linkage specificity, which underscores the specificity of our antibody and approach.

We validated these results by affinity-purification coupled to Western blotting, which confirmed the strong interaction of K11/K48-linked chains with endogenous p97, BAG6, UBQLN2, p62, UBR5, and HUWE1 (Figure 4B). BAG6, p62 and UQBLN2 bound K11/K48-linked chains only if new proteins were synthesized, while the E3s UBR5 and HUWE1 were enriched in the presence of cycloheximide. The latter behavior is expected if the purification of E3 ligases was due to automodification with K11/K48-linked chains. Reciprocal affinity- purification of proteasome and p97/VCP receptors, or endogenous BAG6, p62, or p97/VCP, confirmed that these proteins efficiently precipitated K11/K48-linked chains (Figure 4C; Figure S5A, B), and as seen upon expression of ubiquitin-TEV, proteasome and p97/VCP adaptors interacted efficiently with branched ubiquitin chains (Figure S5C). BAG6, UBR5, p97/VCP, p62, and HSP90 also accumulated at K11/K48-positive aggregates (Figure 4D; Figure S5D, E), while co-localization was neither seen with a marker of stress granule formation (Figure S5F), nor with unrelated ubiquitin-binding proteins not identified in our proteomic experiments (Figure S5G). Providing further validation, depletion of the BAG6 chaperone increased the abundance of puromycylated proteins and extended the time needed for their clearance (Figure S5H).

Among the candidate components of this quality control network, we were intrigued by the small number of E3 ligases that were enriched in K11/K48-specific affinity-purifications (Figure 4A). This observation raised the possibility that we could identify the major enzymes responsible for K11/K48-branched chain production during proteotoxic stress. Indeed, by depleting combinations of candidate E3s we found that loss of both UBR4 and UBR5, using multiple siRNA sequences to ensure on-target specificity, was sufficient to inhibit the formation of most K11/K48-linked chains in cells with proteotoxic stress (Figure 5A; Figure S6A). The same treatment strongly stabilized puromycylated proteins (Figure 5B). By contrast, depletion of Listerin or the APC/C-E2 UBE2S, which were not enriched in our proteomic studies, did not affect production of K11/K48-branched chains and did not

prolong the half-life of puromycylated proteins (Figure S6B–D). As UBE2S was required for K11/K48-linked chain formation during mitosis (Figure 2B), these results highlight that different enzymes produce K11/K48-linked chains during mitosis and upon proteotoxic stress, respectively.

To ascertain whether UBR4 and UBR5 synthesize K11/K48-linked chains, as suggested by these genetic analyses, we used CRISPR/Cas9 genome editing to integrate a FLAG-epitope into the *UBR4* and *UBR5* loci. This allowed us to purify endogenous complexes containing these E3 ligases and interrogate them for their ubiquitylation activity and specificity. Importantly, both UBR4 and UBR5 complexes synthesized K11/K48-linked chains *in vitro*, with the HECT-E3 UBR5 being the more efficient enzyme (Figure 5C). Incubation with mixtures of ubiquitin^{K11R} and ubiquitin^{K48R} suggested that UBR5 produced branched ubiquitin chains, as seen in cells (Figure 3B), while UBR4 appeared to synthesize mixed chains containing multiple linkages (Figure 5C; Figure S6E). We confirmed the very efficient formation of branched ubiquitin conjugates by UBR5 using the ubiquitin-TEV assay (Figure 5D) and directly showed that UBR5 cooperated with a K11-specific enzyme to produce K11/K48-branched trimers (Figure 5E). By using single-Lys ubiquitin mutants, we noted that endogenous UBR5 displayed a striking preference for Lys48 of ubiquitin (Figure 5F), suggesting that it produces branched conjugates that contain multiple blocks of K48-linked chains.

Having reconstituted K11/K48-branched chain formation allowed us to analyze detection of these conjugates by ubiquitin effectors. Thus, we used UBR5 to generate either K11/K48-branched or homotypic K48-linked polymers, and incubated these conjugates with immobilized proteasomal or p97/VCP substrate adaptors. Similar to mitotic K11/K48-branched chains (Meyer and Rape, 2014), we found that the proteasomal substrate adaptor HHR23A and the p97/VCP adaptor NSFL1/p47, both identified as effectors in our proteomic analysis, bound K11/K48-branched chains with much higher affinity than homotypic K48-linked chains (Figure 5G; Figure S6F). Consistent with these results, proteasome inhibition strongly stabilized both puromycylated proteins and K11/K48-linked chains in cells (Figure 5H). Thus, UBR4 and UBR5 are key quality control E3 ligases that decorate targets with K11/K48-branched chains to allow for efficient substrate recognition by the segregase p97/VCP and the 26S proteasome.

K11/K48-specific quality control is linked to neurodegenerative diseases

Recent CRISPR/Cas9 screens had identified components of K11/K48-specific quality control, including the E3s UBR4 and UBR5, as essential proteins in human cells (Wang et al., 2015b), and deletion of *UBR4* or *UBR5* in mice resulted in early lethality (Saunders et al., 2004; Tasaki et al., 2013). In addition, mutations in enzymes or effectors of this quality control network had been linked to neurodegenerative diseases, such as ALS, Huntington's Disease, or ataxia (Figure S7A). This implied that K11/K48-specific quality control is an essential pathway that might prevent the accumulation of neurotoxic proteins. To test this notion, we focused on Huntington's Disease (HD), which is caused by CAG-repeat expansions in *HTT* that produce a Huntingtin (HTT) protein with more than 35 glutamine residues in its amino-terminal domain. UBR5 was recently identified as a candidate genetic

modifier for the age of onset of HD (Genetic Modifiers of Huntington's Disease, 2015). Repeat-associated non-ATG translation of HTT yields peptides that resemble BAG6 substrates (Banez-Coronel et al., 2015), and HTT aggregation increases levels of K11- and K48-linkages attached to unknown substrates (Bennett et al., 2007). Most importantly, an investigation of K11/K48-ubiquitylated proteins revealed modification of endogenous HTT at Lys337 in four independent experiments.

Consistent with these observations, aggregates of pathological 73Q-HTT were strongly decorated with K11/K48-linked chains in cancer cells, embryonic stem cells, or differentiated neurons (Figure 6A–C). The expression of 73Q-HTT, but not benign 23Q-HTT, also induced an overall increase in K11/K48-linked chains in these cells (Figure S7B). Similar observations were made without overexpression in brains of an HD mouse model (Langfelder et al., 2016), where 175Q-HTT aggregates were labeled with K11/K48-linked conjugates (Figure 6D). Thus, the K11/K48-bispecific antibody not only detects its epitope in biochemical experiments or cell culture, but also in tissues. Denaturing purification of HTT as well as native precipitation of ubiquitin chains strongly suggested that 73Q-HTT, but less so 23Q-HTT, was modified with K11/K48-linked chains (Figure 6E; Figure S7C), which was reduced by co-depletion of UBR4 and UBR5 (Figure S7D). By combining denaturing purification of HTT with expression of ubiquitin-TEV, we found that 73Q-HTT, but not 23Q-HTT, was modified with branched chains (Figure 6F). In line with these results, 73Q-HTT bound BAG6 (Figure S7E), and BAG6, UBQLN2, p62 and p97 were efficiently recruited to K11/K48-positive aggregates of 73Q-HTT (Figure 6G). In contrast to 73Q-HTT, ALS-causing FUS variants were not labeled with K11/K48- linked chains under these conditions (Figure S7F). We conclude that pathological HTT variants, but not all aggregation-prone proteins, are processed by K11/K48-specific quality control.

These results raised an intriguing possibility for how aggregation-prone proteins could accelerate the progression of neurodegenerative disorders: if the load capacity of K11/K48-specific quality were limited, expression of pathological HTT might negatively impact processing of newly synthesized proteins, and *vice versa*. To test this possibility, we expressed 73Q-HTT to form K11/K48-positive aggregates in hESCs or neurons. We then inhibited the proteasome or HSP70 to stabilize misfolded nascent polypeptides, and asked whether accumulation of the latter quality control substrates affected the ubiquitylation or processing of 73Q-HTT. Strikingly, proteasome or HSP70 inhibition caused the redistribution of K11/K48-linked chains from 73Q- HTT to distinct aggregates, which was dependent on ongoing protein synthesis (Figure 7A, B; Figure S7G). Other components of K11/K48-specific quality control followed the ubiquitin signal: while BAG6 and UBQLN2 marked 73Q-HTT aggregates in control cells, co-localization was lost upon HSP70 or proteasome inhibition, and production of new proteins was required for this effect (Figure 7C). The redirection of K11/K48-linked chains towards nascent proteins diminished the ability of cells to counteract aggregation: depletion of BAG6 not only delayed clearance of puromycylated proteins (Figure S5H), but also increased the number of 73Q-HTT foci (Figure 7D). Thus, 73Q-HTT and newly synthesized proteins compete for a limited pool of enzymes or effectors of the essential K11/K48-specific quality control machinery.

Discussion

The recent biochemical discovery of heterotypic ubiquitin chains and their potential roles in mitosis and inflammatory signaling raised the possibility that cells use combinations of multiple ubiquitin linkages to encode biological information. However, in the absence of any method to follow physiological mixed or branched chains, i.e. without *in vitro* reconstitution, purification of ubiquitin chains from lysates, or expression of engineered ubiquitin variants, the abundance and physiological relevance of complex ubiquitin chain types remained poorly understood. To address this gap in our understanding of ubiquitin-dependent signaling, we established bispecific antibodies that detect endogenous K11/K48-linked chains in cells. As demonstrated here, such antibodies allow for identification of signaling events regulated by heterotypic chains; discovery of ubiquitylation substrates, enzymes, and effectors; and diagnostic monitoring of aberrant ubiquitin signaling associated with human pathologies. Bispecific antibodies therefore provide a means to dissecting the increasing complexity of ubiquitin-dependent signaling.

Substrates of K11/K48-branched ubiquitin chains

Having a tool in hand to follow the formation of K11/K48-linked chains, we found that heterotypic conjugates target mitotic regulators and misfolded nascent polypeptides for degradation. These findings place K11/K48-linked chains at the heart of cell cycle and protein quality control, two conditions that rely on high proteasome activity: while the APC/C ensures that a large number of substrates are turned over during the short time span of mitosis (Sivakumar and Gorbsky, 2015), translation-coupled quality control triages up to 15% of newly synthesized proteins (Balchin et al., 2016; Harper and Bennett, 2016; Wang et al., 2015a; Wang et al., 2013). Even though the architecture of K11/K48-branched chains differs during mitosis and quality control (Figure 7E), physiological and biochemical evidence suggests that both types of K11/K48- branched chains afford a higher affinity towards the proteasome and its associated segregase p97/VCP than homotypic K11- or K48-linked conjugates (Meyer and Rape, 2014). While we do not wish to exclude mechanisms of branch recognition, we speculate that the higher affinity of p97/VCP and proteasomal receptors towards K11/K48-branched chains is due to a branching- dependent increase in the local concentration of proteolytic ubiquitin chains. We propose that K11/K48-branched chains are proteasomal priority signals that allow cells to rapidly clear specific proteins.

As we have started to dissect the mechanism of substrate recognition during K11/K48-specific quality control, it is interesting to note that chaperones bind misfolded proteins through extended hydrophobic stretches (Balchin et al., 2016; Hartl et al., 2011). Structural studies showed that the APC/C also recognizes its mitotic targets through extended low complexity motifs referred to as D- or KEN-boxes (Brown et al., 2016; Chang et al., 2015). In addition, mitotic regulators are often incorporated into stable complexes (Huttlin et al., 2015), and misfolded proteins rapidly engage in oligomeric interactions *en route* to aggregation (Bemporad and Chiti, 2012). These parallels might explain a striking overlap between the enzymes of cell cycle and protein quality control: while the APC/C was identified as an E3 ligase that prevents protein aggregation in *C. elegans* (Brehme et al., 2014), the quality control E3 UBR5 *vice versa* binds the APC/C and regulates the spindle

checkpoint (Scialpi et al., 2015). Moreover, p97/VCP, an effector of K11/K48-specific quality control, was originally identified as a cell division cycle mutant (Moir et al., 1982). It therefore appears that different pathways converged on ubiquitin chain branching as a common solution to the need for efficient turnover of difficult or abundant proteasome substrates (Figure 7E).

Enzymes of K11/K48-linked ubiquitin chain formation

Consistent with *in vitro* studies (Meyer and Rape, 2014), we identified the APC/C as the major E3 ligase for the production of K11/K48-branched chains during mitosis (Figure 7E). The ability of the APC/C to synthesize such conjugates depends on UBE2S, an E2 enzyme that branches blocks of ~6–7 K11-linked subunits off chains initiated by UBE2C or UBE2D (Meyer and Rape, 2014; Wickliffe et al., 2011). Two different E3 ligases, UBR4 and UBR5, carry the main load of K11/K48-linked chain synthesis during proteotoxic stress (Figure 7E). Co-depletion of UBR4 and UBR5 eliminated most K11/K48-linked chains during quality control and strongly inhibited the proteasomal degradation of puromycylated proteins. Reconstitution assays revealed that UBR4- and UBR5-complexes efficiently synthesize K11/K48-linked chains, with UBR5 likely branching multiple K48-linked chains off substrates initially modified with mixed conjugates. The key enzymes of K11/K48-linked chain synthesis highlight the importance of such conjugates for signaling, as the APC/C, UBR4, and UBR5, are all essential in metazoans (Saunders et al., 2004; Sivakumar and Gorbsky, 2015; Tasaki et al., 2013; Wang et al., 2015b).

It is interesting to note that UBR4 and UBR5 are distinct from ubiquitylation enzymes that had previously been implicated in proteostasis, including Listerin, which targets nascent polypeptides on stalled ribosomes (Bengtson and Joazeiro, 2010; Brandman et al., 2012; Shao et al., 2015); CHIP, which ubiquitylates clients of the HSP70 and HSP90 chaperones (Meacham et al., 2001; Scaglione et al., 2011); HUWE1, which helps degrade proteins that fail to engage an obligate binding partner (Sung et al., 2016; Xu et al., 2016); or the yeast UBR1 and SAN1, which modify unfolded proteins in the cytoplasm and nucleus, respectively (Gardner et al., 2005; Shemorry et al., 2013). This suggests that the quality control machinery discovered here complements known pathways that ensure proteostasis in human cells. The enzymes and effectors of K11/K48-specific quality control appear to be well suited to safeguard new protein synthesis: UBR5 contains an RNA-binding domain that might direct it to translating polysomes, while effectors of this pathway, such as BAG6, p97, and the proteasome, frequently operate in association with the ribosome (Brandman et al., 2012; Hessa et al., 2011; Rodrigo-Brenni et al., 2014; Sha et al., 2009; Turner and Varshavsky, 2000; Verma et al., 2013). These observations imply that K11/K48-specific quality control immediately checks the integrity of newly synthesized proteins to prevent their deleterious aggregation.

K11/K48-linked chains and neurodegeneration

In addition to newly synthesized proteins, K11/K48-branched chains also decorate pathological variants of HTT, and enzymes and effectors of K11/K48-linked conjugates are mutated in neurodegenerative diseases, including HD (Genetic Modifiers of Huntington's Disease, 2015; Weishaupt et al., 2016). As the proteasome is unable to clear aggregates, we

expect soluble oligomeric HTT to be the major target of K11/K48-specific quality control; the neurotoxicity of the this oligomeric HTT species (Miller et al., 2011) might explain why this substrate is modified with a proteasomal priority signal that ensures its rapid clearance from cells. As the load capacity of the K11/K48-specific network to handle both nascent polypeptides and pathological HTT is limited, neurotoxic proteins could exert their effects by allowing the accumulation of newly synthesized, misfolded proteins that in turn impede multiple cellular pathways. Consistent with this idea, inhibition of protein synthesis, a condition that reduces the burden for K11/K48- specific quality control, ameliorated phenotypes of protein aggregation (Das et al., 2015), while expression of mutant HTT, a condition that exacerbates the need for the K11/K48-specific pathway, caused misfolding of other metastable proteins in *C. elegans* (Gidalevitz et al., 2006). Although more work is required to investigate the crosstalk between substrates, our results raise the possibility that activators of K11/K48-specific quality control could provide therapeutic benefit against neurodegenerative disorders.

In summary, by developing a method to detect and purify K11/K48-linked chains, we revealed roles for endogenous heterotypic ubiquitin polymers in cell cycle and protein quality control. Ubiquitin contains eight sites for polymer formation, and cells could assemble 28 distinct chain types with two linkages and a large number of more complex conjugates. Even if few combinations exert specific functions, ubiquitin-dependent signaling is likely to be more complex than anticipated, yet our work describes a powerful strategy to decipher this essential system for cellular information transfer.

STAR METHODS

Contact for Reagent and Resources Sharing

Further information and requests for reagents and resources should be directed to the Lead Contact Michael Rape (mrape@berkeley.edu).

Experimental Model and Subject Details

Mammalian cell culture and stable cell lines—Human embryonic kidney (HEK) 293T cells and HeLa cells were maintained in Dulbecco's Modified Eagle's Medium (DMEM) supplemented with 10% FBS. Cells were routinely screened for mycoplasma contamination. Plasmids transfections were either with calcium phosphate precipitation method or with polyethylenimine (PEI). Lentiviruses were produced in 293T cells by cotransfection of lentiviral constructs with packaging plasmids (Addgene) forand was harvested 48 and 72 hours post-transfection. Stable cell lines were maintained in DMEM media supplemented with 10% Tet- FBS. To induce expression of stably transfuced Htt-GFP constructs, media was supplemented with 1μg/ml Doxycylcine.

Human embryonic stem cell culture and differentiation—Human embryonic stem (hES) H1 cells (WA01) were maintained under feeder free conditions on Matrigel-coated plates (#354277, BD Biosiences) in mTeSRTM1, (#05871/05852, StemCell Technologies Inc.) with daily medium change. They were routinely passaged with collagenase (#07909, StemCell Technologies Inc.) and ReLesR (#05872, StemCell Technologies Inc.). For

transduction, single cell suspensions were prepared by treatment of hES cells with accutase (#07920, StemCell Technologies Inc.) and 0.5×106 hES H1 cells per well of a 6-well were centrifuged with lentiviruses in the presence of 6 μg/ml Polybrene (Sigma) and 10 μM Y-27632 ROCK inhibitor (Calbiochem) at 1000g at 30°C for 90 min. After spinfection, media was changed to mTeSRTM1 supplemented with 10 μM Y-27632 ROCK inhibitor (Calbiochem). hES H1 cells were selected with appropriate antibiotic (200 μg/ml G418 for pINDCUER20) for 7 days and used in experiments.

For differentiation into neural progenitor cells, hES H1 cells were subjected to a neural conversion protocol using STEMdiffTM Neural Induction Medium (#05831, StemCell Technologies Inc.) and a monolayer culture method according to the manufacturer's guidlines (#28044, StemCell Technologies Inc.) and as previously described (Chambers et al 2009). In brief, single cell suspensions were prepared by treatment of hES cells with accutase (#07920, StemCell Technologies Inc.) and 2.0×106 cells were seeded per well of a 6-well plate in STEMdiffTM Neural Induction Medium supplemented with 10 μM Y-27632 ROCK inhibitor. Neural conversion was performed with daily medium change. At day 6 of differentiation cells were split on Matrigel-coated coverslips for fluorescence microscopy analysis at day 9. For differentiation into neurons, hES H1 cells subjected to neural conversion for 6 days as described above, passaged, and maintained in DMEM F12 containing 1x B-27® Supplement (17504044, Gibco) to promote spontaneous differentiation into neurons ((#28044, StemCell Technologies Inc.). At day 20 of differentiation cells were split on Matrigel-coated coverslips for fluorescence microscopy analysis at day 25. For hES H1 cells transduced with pINDCUER20 constructs, expression of the transgenes was induced by adding 1ug/mL doxycyclin to the media for 72h before immunoblot or immunofluorescence analysis.

Method Details

Bispecific Antibody Cloning—Bispecific antibodies were generated using knobs-into-holes heterodimerization technology24. The heavy chain variable domains of the previously described anti-K11 polyubiquitin linkage- specific antibody (clone 2A3/2E6)23, the anti-K48 polyubiquitin linkage-specific antibody (clone Apu2.07)22, and a non-specific anti-gD control antibody were subcloned into a modified pRK vector (Genentech) containing the human IgG1 heavy chain constant domains with either the knob (T366W) or hole (T366S, L368A, and Y407V) mutations in the CH3 domain. The light chain variable domains were similarly subcloned into a modified pRK vector (Genentech) containing the human kappa light chain constant domain. The pRK vector carries a constitutive strong signal peptide for extracellular expression in mammalian cells. For this study, the anti- K11 antibody was cloned as both knob and hole mutants, the anti-K48 was cloned as a hole mutant, and the anti-gD was cloned as a knob mutant.

Knob and Hole Half Antibody Expression, Purification, and Annealing—The knob and hole half antibodies were expressed separately in CHO cells and isolated individually. Light chain and heavy chain plasmids for a given knob or hole half antibody were transiently co-transfected into CHO cells using PEI as previously described60. Half antibodies were purified over MabSelect SuRe resin (GE Healthcare), eluted with 50 mM

sodium citrate, 150 mM NaCl, pH 3.0, followed by pH adjustment to 5.0 with 10% (v/v) of 200 mM arginine, 137 mM succinate, pH 9.0.

Bispecific antibodies were assembled in vitro using a modified version of the previously described method of annealing, reduction, and oxidation61. Briefly, the desired knob and hole half antibodies were mixed at a 1:1 mass ratio and the pH of the mixture was adjusted to 8.5 with 15% (v/v) of 800 mM arginine, pH 10.0. A 200-fold molar excess of reduced glutathione (Sigma Aldrich) in 800 mM arginine, pH 10.0 was added and the assembly reaction was incubated at room temperature for 72 hours with exposure to air to allow annealing of the knob and hole half antibodies and formation of the hinge disulfides.

Bispecific Antibody Purification—Assembled bispecific antibodies were purified by hydrophobic interaction chromatography (HIC). Briefly, the assembly reaction was conditioned with 3 volumes of buffer A (25 mM sodium phosphate, 1 M ammonium sulfate, pH 6.5) to a final concentration of 0.75 M ammonium sulfate. The assembly reaction was filtered, loaded onto a 5 μm, 7.8×75 mm ProPac HIC-10 column (Dionex), followed by washing with buffer A. A 0–100% buffer B (25 mM sodium phosphate, pH 6.5, 25% isopropanol) linear gradient over 40 column volumes (CVs) was performed to separate the bispecific antibody from any unreacted half antibodies or aggregated protein. Identity of the eluting peaks was monitored by SDS-PAGE and mass spectrometry (see below for method details).

The bispecific antibodies were further purified by cation-exchange chromatography (CEX). Briefly, the HIC pooled material was dialyzed into 20 mM sodium acetate, pH 5.0, loaded onto a 10 μm Mono S 5/50 GL column (GE Healthcare), and washed with buffer A (20 mM sodium acetate, pH 5.0). A 0–100% buffer B (20 mM sodium acetate, pH 5.0, 1 M NaCl) linear gradient over 40 CVs was performed and the desired fractions pooled. The purified bispecific antibodies were formulated in 20 mM histidine acetate, 240 mM sucrose, 0.02% Tween-20, pH 5.5.

SEC-MALS—50 μg of antibody was injected onto a 3.5 μm, 7.8 mm×300 mm XBridge Protein BEH analytical SEC 200 Å column (Waters) at 1 mL/min using an Agilent 1260 Infinity HPLC with 20 mM histidine acetate, 300 mM NaCl, pH 5.5 as the mobile phase. Proteins eluted from the analytical SEC column were directly injected onto a Wyatt DAWN HELEOS II/Optilab T-rEX multi-angle light scattering detector to measure molar mass and polydispersity.

Mass Spectrometry—30 μg of antibody was deglycosylated with 2 units of PNGaseF (NEB) in the presence or absence of 2 units of carboxypeptidase B (Roche) at 37 °C overnight prior to mass spectrometry analysis. 2 μg of antibody was then injected onto a 3 μm, 4.6×50 mm reverse-phase chromatography PLRP-S column (Agilent) at 1 mL/min using an Agilent 1290 Infinity UHPLC. A 0–100 % buffer B gradient over 3 minutes was performed with 0.05 % trifluoroacetic acid (TFA) in water (buffer A) and 0.05 % TFA in acetonitrile (buffer B), followed by a 100 % buffer B wash for 1 minute. Proteins eluted from the reverse-phase column were directly injected onto an Agilent 6230 electrospray ionization time-of-flight mass spectrometer (ESI-TOF) for intact mass measurement.

Fluorescent Labeling of Antibodies—The anti-K11 monospecific antibody and the anti-K11/K48 bispecific antibody were labeled with Alexa Fluor® 488 and Alexa Fluor® 546, respectively, according to the manufacturer's instructions using Alexa Fluor® Protein Labeling Kits (ThermoFisher). Unreacted free dye was removed through extensive dialysis. Six and 8 moles of Alexa Fluor® 488 and Alexa Fluor® 546, respectively, per mole of antibody was conjugated.

Surface Plasmon Resonance—Affinities of the antibodies were determined by surface plasmon resonance (SPR) using a BIACORE 3000 system (GE Healthcare). Ubiquitin proteins were immobilized on CM5 sensor chips (GE Healthcare) using the amine-coupling method with different surface densities denoted by the difference in resonance units (RUs). The 1:1 diubiquitin mixture was generated by mixing K11- and K48-linked diubiquitin in an equimolar ratio, followed by immobilization on the sensor chip. All analytes were tested in the IgG format to demonstrate avidity. Analytes were run at the indicated concentrations in HBS-P buffer (0.01 M HEPES, 0.15 M NaCl, and 0.005% v/v surfactant P20, pH 7.4). For the K11/K48 bispecific, K11 monospecific, and K48 monospecific antibodies, concentrations of 10 nM, 5 nM, 2.5 nM, 1 nM and 0 nM (buffer alone) were run in duplicate. For the K11/gD and K48/gD bispecific control antibodies concentrations of 50 nM, 30 nM, 10 nM, 5 nM, 1 nM, and 0 nM (buffer alone) were run in duplicate. Following a dissociation period of 600 seconds, the chip surface was regenerated with 40 mM HCl. All Biacore sensorgrams were analyzed with the Biaevaluation 4.1 software (GE Healthcare). All experimental refractive index measurements were normalized by subtraction of the reference flow cell responses. Representative measurements from three independent experiments of the kinetic constants and binding constants are shown.

In vitro transcription/translation—^{35}S-labeled cyclin A was synthesized by incubating pCS2-cyclin A plasmids in rabbit reticulocyte lysates (RRL) in the presence of ^{35}S-Met for 2 hours at 30°C. ^{35}S-labeled cyclin A was used as a substrate for the APC/C in in vitro ubiquitylation assays as described. The reaction was terminated via the addition of urea buffer (8M urea, 2% Triton-X100, 20mM Tris pH 7.5, 135mM NaCl, 1mM EDTA, 1.5mM MgCl2, and 10% glycerol supplemented with 10mM N-Ethylamine and protease inhibitors (Roche)) and was then supplemented with an equal volume of lysis buffer without urea or Triton X-100. Immunoprecipitations were performed as described above using the indicated antibodies and analyzed via SDS-page and autoradiography. Signals were quantified using ImageJ software.

Immunofluorescence microscopy—For immunofluorescence analysis, HeLa cells were seeded on coverslips and fixed with 4% paraformaldehyde for 15 min, permeabilized with 0.3% Triton X-100 for 30 min. Cells were blocked with 2% BSA, 0.1% Triton X-100. hES H1 cells were seeded on Matrigel-coated coverslips using accutase, fixed with 3.7% formaldehyde for 10 min, permeabilized with 0.3% Triton for 20 mins. After fixation and permeabilization, cells were stained with indicated antibodies or Hoechst. Images were taken using Zeiss LSM 710 confocal microscope and processed using ImageJ.

For quantification of K11/K48 positive aggregates, Hela cells were treated with MG132 or MG132 and cycloheximide for different time spans and were imaged using the 60x objective

of the Zeiss LSM 710 confocal microscope. The number of cells containing K11/K48 positive aggregates was counted; the number of aggregates and their size were determined using the count particle function in ImageJ. To analyze the number of 73Q-HTTGFP inclusion bodies and the number of 73Q-HTTGFP inclusion bodies modified with K11/48 heterotypic chains, 73Q- HTTGFP-expressing hES H1 cells were subjected to indicated drug or siRNA treatments, stained them with K11/48-bispecific antibodies, and analyzed them by indirect immunofluorescence microscopy. Images were taken for each condition using a Zeiss LSM 710 confocal microscope with a 20x objective followed by quantification of the average number of 73Q-HTT inclusion bodies per frame (green channel) and average number of K11/48-positive 73Q-HTT inclusion bodies per frame (red channel) using the count particle function in ImageJ. The average number of K11/48-positive 73Q-HTT inclusion bodies per frame was normalized to the average number of 73Q-HTT inclusion bodies per frame. Error bars represent standard deviation of the mean of at least three biological replicates (>10 frames each containing >200 cells were counted per replicate).

Immunohistochemistry—For double-staining of mHtt aggregates and K11/K48-linked chains in mouse brain samples, 40μm coronal sections of 6-month Q175 HD Knock-in mice or WT mice were washed in PBS and blocked with 3% bovine serum albumin and 2% normal goat serum (Vector Labs) in PBS with 0.2% Triton X-100 at room temperature for 1 hour. Sections were then incubated with anti- huntingtin protein antibody (clone mEM48, 1:150; Millipore MAB5374) and K11/K48 antibody (1:500) in blocking buffer overnight at 4 degree. After three 10-min washes in PBS with 0.1% Triton X-100, the sections were incubated with biotinylated goat anti-mouse antibody (1:300) (Vector Labs) for 2h at room temperature. Following another three 10-min washes, the sections were incubated for 2h with anti-human-488 (1:300) and Streptavidin, Alexa Fluor 594 conjugate (1:300, Thermo Fisher Scientific) in blocking buffer. The sections were washed again and mounted with antifade mounting medium with DAPI (Vector Labs).

Cellular stress assays—To identify conditions of K11/K48-linked chain formation HEK 293T or HeLa cells were treated with different drugs: Epoxomycin (1μM, 6h, Sigma-Aldrich), MG132 (10μM, 6h, Sigma-Aldrich), Pifithrin μ (10μM, 6h, Sigma-Aldrich), VER155008 (40μM, 6h, Sigma-Aldrich), 17 DMAG (1μM, 6h, Sigma-Aldrich), Chloroquine (100μM, 6h, Abcam), DBEQ (10μM, 6h, Sigma-Aldrich), Oligomycin/ Antimycin (each 10μM, 1h, Sigma-Aldrich), CCCP (10μM, 2h, Abcam), Cycloheximide (100μg/mL, 6h, Sigma-Aldrich), Puromycin (25μM, 1h, Sigma-Aldrich), DTT (2mM, 6h), Tunicamycin (10μg/mL, 2h, Sigma-Aldrich), Doxorubicin (5μM, 6h, Sigma-Aldrich). Translation and transcription inhibitors were used at the following concentrations: Cycloheximide (100μg/ml), Harringtonine (2μg/ml), Emetine (20μg/ml), Puromycin (1μg/ml), α- Amanitin (5μg/ml). Accumulation of K11/K48-linked chains was monitored by Western blot or immunofluorescence microscopy.

Cell synchronization—HeLa cells were first synchronized in S-phase with 2 mM thymidine for 24h. Cells were then washed with PBS and released into fresh DMEM/10% FBS media for 3h. Finally, cells were treated with 10ng/ml nocodazole or 5μM STLC for 11h and arrested in prometaphase. For progression through mitosis, cells were harvested via

pipetting, washed with PBS, and released into fresh media. Samples were taken at indicated time points and analyzed via western blot. For proteasome inhibition, cells were released from prometaphase for 90min to silence the spindle checkpoint before treatment with 20μM MG132. For Ube2S depletion, cells were first transfected with 10nM Ube2S or control siRNA as described above, 24h prior to synchronization.

CRISPR/Cas9 Genome editing—FLAG-UBR4 and FLAG-UBR5 HEK293T cell lines were generated using single-guide RNA- encoding plasmid derivatives of pX330-U6-Chimeric_BB-CBh-hSpCas9 and single-strand donor DNA. HEK293T cells were transfected with pX330 derivative and single stranded donor oligo using Mirus *Trans*IT-293 Transfection reagent and individual clones were expanded in 96-well plates. Homozygous clones were screened by PCR, DNA sequencing and confirmed by western blot analysis.

Immunoprecipitations—Immunoprecipitations were performed from lysates of mitotic HeLa cells with or without MG132 or from HEK 293T cells treated with MG132/Pifithrin-μ or MG132/Pifithrin-μ and cycloheximide. Cell pellets were resuspended in 2 volumes swelling buffer (SB) (50mM HEPES pH7.5, 1.5mM MgCl2, 5mM KCl) supplemented with 10mM N-Ethylamine and protease inhibitors (Roche) on ice. Lysis was performed by two freeze/thaw cycles in liquid nitrogen and multiple passages through a 25G 5/8 needle. Lysates were cleared by centrifugation. Extracts were supplemented with 150mM NaCl and 0.1% Tween-20, normalized to 280nm absorption readings, and incubated with the indicated antibodies bound to protein-G agarose beads for 3h at 4°C. After washing with lysis buffer, bound proteins were eluted with 2x SDS sample buffer and analyzed by immunoblotting. For detecting HUWE1, Ubr5, Bag6, p97, p62, and ubiquilin2 binding in immunoprecipitations experiments using linkage-specific antibodies, extracts were supplemented with 250mM NaCl and 0.15% Tween-20. For HA-tag immunoprecipitations, HEK293T cells were transfected with plasmids encoding indicated HA-tagged proteasome and p97 adaptors and lysed in 20mM HEPES ph7.5, 150mM NaCl, and 0.2% NP-40 buffer supplemented with 10mM N-Ethylamine and protease inhibitors (Roche). Lysates were clarified via centrifugation and incubated with anti-HA resin. After washing with lysis buffer, immune- complexes were eluted in 2x sample buffer and analyzed via immunoblotting. Denaturing immunoprecipitations were performed as previously described (Meyer and Rape, 2014). Briefly, cells were re-suspended in lysis buffer (8M urea, 1% Triton-X100, 20mM Tris pH 7.5, 135mM NaCl, 1mM EDTA, 1.5mM MgCl2, and 10% glycerol supplemented with 10mM N-Ethylamine and protease inhibitors (Roche)) and sonicated. Lysates were supplemented with an equal amount of lysis buffer with no urea, and centrifuged. Supernatants were pre-cleared and incubated with protein G beads coupled with the indicated antibodies. Beads were then washed and bound proteins were eluted with urea sample buffer and analyzed by immunoblotting.

HIS-tag pulldowns—HEK 293T cells transfected with plasmids encoding HIS6-tagged Htt constructs were lysed under denaturing conditions (8M urea, 1% Triton-X100, 50mM Tris pH 8, 50mM Na_2HPO_4, 300mM NaCl, and 10mM imidazole, supplemented with 10 mM N-Ethylamine and protease inhibitors (Roche)). After sonication, lysates were incubated with Ni-NTA agarose beads for 2h at room temperature. After washing with lysis

buffer, bound proteins were eluted in sample buffer supplemented with 6M urea and 250mM imidazole, and analyzed via immunoblotting.

Detection of branched ubiquitin chains with ubiquitin TEV derivates—Detection of branched ubiquitin chains in cells was performed as described 9. To detect branched chains synthesized during proteotoxic stress, HEK 293T cells expressing FLAGubiquitin53TEV and His-ubiquitin64TEV/FLAG were treated with MG132 or MG132 and cycloheximide. Cells were then lysed as described above and ubiquitin chains were immunoprecipitated using αK11/K48 or αFK2 antibodies. To detect branched ubiquitin chains on huntingtin, HEK293T cells were transfected with plasmids encoding HIS6-Htt-23Q or HIS6-Htt-73Q with FLAGubqiuitin53 TEV and ubiquitin64TEV/FLAG and denaturing HIS-tag purifications were performed as described above. To detect branched chain modified substrates bound by proteasome or p97 adaptors, HEK293T cells were transfected with HA-tagged HHR23A or UBXD7 with FLAGubqiuitin53 TEV and ubiquitin64TEV/FLAG and treated with MG132. HA-tag immunoprecipitations were performed as described above. After incubation in lysates, beads were washed with lysis buffer followed by TEV cleavage buffer (10mM Tris pH8.0, 150mM NaCl, 0.5mM EDTA, and 1mM DTT) and bound proteins were treated with TEV protease for 2h at 30°C. To detect branched chains synthesized in v itro, in vitro ubiquitylation assays were performed with FLAG-Ubr5 as described above using recombinant FLAGubiquitin53TEV and His-ubiquitin64TEV/FLAG. TEV protease was added directly to the in vitro ubiquitylation reaction mixture. N-Ethylamine was excluded from all buffers. Reactions were resolved by 18% Tricine-SDS-PAGE gels and immunoblotting.

Puromycin pulse-chase assays—HEK 293T cells were treated with 5μg/ml puromcyin for 1h. After 2 washes with PBS, cells were released into fresh media supplemented with either cycloheximide alone or cycloheximide plus MG132. Where indicated, siRNA transfections were performed 24h prior to puromycin treatments. Cells were harvested and lysed in sample buffer at the time points indicated and proteins were analyzed via immunoblotting.

Immunoprecipitations for mass spectrometry—Synchronized HeLa cells or HEK 293T cells treated with puromycin for 6h were lysed in SB as described above. Lysates were precleared by incubation with protein-G agarose beads for 60 mins at 4°C, divided into 3 samples and incubated w ith K11/K48, K11/gD, or K48/gD antibodies bound to protein-G agarose beads for 90 mins at 4°C . After washing with lysis buffer, bound proteins were denatured with 8M urea/ 100mM Tris pH8.5, and treated with 5mM TCEP and 10mM iodoacetamide. An on-bead digestion with 0.5 mg/mL trypsin was performed over night at 37°C before the samples were processed for multidim ensional protein identification technology (MUDPIT) mass spectrometry.

Protein purification—Except for Human E1, His6-tagged proteins were purified from BL21/DE3 (RIL) cells. Cells were grown in LB-medium to OD600nm 0.5. Protein expression was induced with the addition of 0.5 mM IPTG and grown at 16°C overnight. Cells were res uspended in lysis buffer (50 mM sodium phosphate, pH 8, 500 mM NaCl, and

10 mM imidazole) and lysed by incubation with 200 mg/ml lysozyme and sonication. Lysates were cleared by centrifugation at 12,500 rpm 4°C for 20 mins. Clarified lysates were incubated with NiNTA (QIAGEN) for 4h at 4°C. Beads were washed with lysis buffer containing 0.1% Triton X-100. Proteins were eluted in 200 mM imidazole in 50 mM sodium phosphate, pH 8, 500 mM NaCl. Enzymes were dialyzed overnight into PBS, 2 mM DTT and all other proteins were dialyzed in PBS alone. MBP-tagged p97 protein was isolated using amylose resing (NEB); purification was performed as described above for His-tagged proteins with lysis buffer consisting of 20 mM Tris-HCl pH 7.5, 500 mM NaCl. Beads were washed with lysis buffer containing 0.1% Triton X-100. Proteins bound to beads were stored at 4°C in PBS supplemented with 5% glycerol and 2mM DTT. Human E1 was expressed purified from ES Sf9 cells described above and buffers were supplemented with 10% glycerol. For untagged ubiquitin purification, BL21/DE3 cells were resuspended in lysis buffer (75 mM Tris, pH 8, 150 mM NaCl, 0.4% Triton X-100, 2 mM EDTA, 8 mM beta-mercaptoethanol, and Roche protease inhibitor cocktail) and lysed with 200 mg/ml lysozyme and sonication. Perchloric acid was added to the clarified lysates and that was then centrifuged again. The supernatant was dialyzed in 50 mM ammonium acetate pH 4.5 overnight and filtered through a 0.22 μm filter. Ubiquitin constructs were purified using a HiTrap SP HP cation exchange column in a 0%-60% NaCl gradient in 50 mM ammonium acetate (pH 4.5) and further purified using size-exclusion chromatography (S75 column, GE Lifescience) in 20 mM Tris-HCl (pH 7.5), 150 mM NaCl.

In vitro ubiquitylation—E3 ligase complexes were immunoprecipitated from cells. For the APC/C, synchronized mitotic HeLa cell lysates were prepared as described above and incubated with anti-Cdc27 coupled protein G beads. For endogenously FLAG-tagged Ubr4 and Ubr5, lysates were prepared as described above for HA-tag immunoprecipitations, and incubated with anti-FLAG resin. Beads were then washed with lysis buffer and then with SB. In vitro ubiquitylation reactions were carried out via incubating E3 ligase coupled beads in UBAB reaction buffer (25 mM Tris-HCl pH 7.5, 50 mM NaCl, 10 mM MgCl2) with 1 μM E1, 1 μM E2 (unless indicated otherwise), 100 μM wildtype ubiquitin or indicated ubiquitin mutants (Boston biochem), 3 mM ATP, 22.5 mM creatine phosphate, 1 mM DTT, and substrates if indicated. N-Ethylamine was excluded from buffers. Reactions were terminated with the addition of 2x sample buffer and boiling samples at 95°C.

For FLAG-Ubr5 and FLAG-Ubr4 immunoprecipitations, cells were lysed in Buffer A (20 mM Hepes pH 7.5, 150 mM NaCl, 0.2% NP-40) supplemented with PMSF, protease inhibitor tablets (Roche), 1mM sodium orthovanadate and 10mM sodium fluoride. Cell lysates were cleared by centrifugation and pre-cleared with protein G beads for 30 min. Immunoprecipitations were performed with FLAG-agarose beads for 2 hours followed by 4 washes in Buffer A. In vitro ubiquitylation reactions were performed by incubating FLAG-Ubr4/5 beads with 1 μM E1, 1 μM UBE2D3, 25 mM wild type ubiquitin or indicated ubiquitin mutants (Boston biochem), 3 mM ATP, 22.5 mM creatine phosphate, and 1 mM DTT in UBAB reaction buffer (25 mM Tris-HCl pH 7.5, 50 mM NaCl, 10 mM $MgCl_2$) in 10 μL total volume. Reactions were terminated with the addition of 2x urea sample buffer and heating samples at 65°C.

When in vitro ubiquitylation reactions were subsequently used for in vitro binding assays with MBP-p97/p47 complexes bound to amylose resin, the in vitro ubiquitylation reactions were terminated and eluted by addition of 30 μL of 20mM N-Ethylmaleimide, 0.1%Triton-X, and 500 ug/mL 3X FLAG peptide in PBS and then added onto MBP-p97/p47 complex bound to amylose resin. Binding reactions were performed at 4°C rota ting and removed at indicated times, washed 4 times with Buffer A and resuspended in 2X urea sample buffer.

Ubiquitin Trimer synthesis—In vitro ubiquitylation reactions were carried out in 1x UBAB buffer with 2 μM E1, 0.1 mg/ml Creatine-phosphate kinase (CPK), 3 mM e-mix, 0.5 mM DTT, and 334 μM Ub-ΔGG. For K11/K63 branched trimers, this reaction was supplemented with 20 μM Ube2S, 20 μM Ube2N, 20 μM Ube2V1, and 666 μM Ub-K11R/K63R. K11/K48 branched trimers were assembled with 20 μM Ube2S, 20 μM Ube2G2, 20 μM gp78, and 666 μM Ub-K11R/K48R. K48/K63 branched trimers were assembled with 20 μM Ube2N, 20 μM Ube2V1, 20 μM Ube2K, and 666 μM Ub- K11R/K48R. Reactions were incubated at 30°C overnig ht. Trimers were purified using a HiTrap SP HP cation exchange column followed by size-exclusion chromatography as described above.

Quantification and Statistical Analysis

Quantitative data are presented as means ± SEM. Extended figure 6d shows a mean of 1–2 biological replicates, all other experiments were independently repeated at least three times. Figure 4a, significant hits had a $p<0.01$ in a s.e.m analysis based on average TSCs. Figures 5e and 5g, at least 10 randomly chosen frames were counted per biological replicate, significance was determined by an unpaired t-test.

Supplementary Material

Refer to Web version on PubMed Central for supplementary material.

Acknowledgments

We thank Julia Schaletzky and Christopher Koth for comments on the manuscripts, and all members of the Matsumoto, Dixit and Rape groups for their discussions, suggestions, and support. We thank Jay Goodman for cloning help. An Otto Bayer Scholarship funded KD. AW is funded by the NIDCR (5K99DE025314). ERC, NMM, MLM, and VMD are employees of Genentech Inc., a member of the Roche Group. MR is supported by an RO1 grant from the NIGMS (5R01GM083064); he also is the Dr. K. Peter Hirth Chair of Cancer Biology at UC Berkeley and an Investigator of the Howard Hughes Medical Institute.

References

Alfieri C, Chang L, Zhang Z, Yang J, Maslen S, Skehel M, Barford D. Molecular basis of APC/C regulation by the spindle assembly checkpoint. Nature. 2016; 536:431–436. [PubMed: 27509861]

Balchin D, Hayer-Hartl M, Hartl FU. In vivo aspects of protein folding and quality control. Science. 2016; 353:aac4354. [PubMed: 27365453]

Banez-Coronel M, Ayhan F, Tarabochia AD, Zu T, Perez BA, Tusi SK, Pletnikova O, Borchelt DR, Ross CA, Margolis RL, et al. RAN Translation in Huntington Disease. Neuron. 2015; 88:667–677. [PubMed: 26590344]

Bemporad F, Chiti F. Protein misfolded oligomers: experimental approaches, mechanism of formation, and structure-toxicity relationships. Chem Biol. 2012; 19:315–327. [PubMed: 22444587]

Bengtson MH, Joazeiro CA. Role of a ribosome-associated E3 ubiquitin ligase in protein quality control. Nature. 2010; 467:470–473. [PubMed: 20835226]

Bennett EJ, Shaler TA, Woodman B, Ryu KY, Zaitseva TS, Becker CH, Bates GP, Schulman H, Kopito RR. Global changes to the ubiquitin system in Huntington's disease. Nature. 2007; 448:704–708. [PubMed: 17687326]

Brandman O, Hegde RS. Ribosome-associated protein quality control. Nat Struct Mol Biol. 2016; 23:7–15. [PubMed: 26733220]

Brandman O, Stewart-Ornstein J, Wong D, Larson A, Williams CC, Li GW, Zhou S, King D, Shen PS, Weibezahn J, et al. A ribosome-bound quality control complex triggers degradation of nascent peptides and signals translation stress. Cell. 2012; 151:1042–1054. [PubMed: 23178123]

Brehme M, Voisine C, Rolland T, Wachi S, Soper JH, Zhu Y, Orton K, Villella A, Garza D, Vidal M, et al. A chaperome subnetwork safeguards proteostasis in aging and neurodegenerative disease. Cell Rep. 2014; 9:1135–1150. [PubMed: 25437566]

Brown NG, VanderLinden R, Watson ER, Weissmann F, Ordureau A, Wu KP, Zhang W, Yu S, Mercredi PY, Harrison JS, et al. Dual RING E3 Architectures Regulate Multiubiquitination and Ubiquitin Chain Elongation by APC/C. Cell. 2016; 165:1440–1453. [PubMed: 27259151]

Chang L, Zhang Z, Yang J, McLaughlin SH, Barford D. Atomic structure of the APC/C and its mechanism of protein ubiquitination. Nature. 2015; 522:450–454. [PubMed: 26083744]

Chau V, Tobias JW, Bachmair A, Marriott D, Ecker DJ, Gonda DK, Varshavsky A. A multiubiquitin chain is confined to specific lysine in a targeted short-lived protein. Science. 1989; 243:1576–1583. [PubMed: 2538923]

Das I, Krzyzosiak A, Schneider K, Wrabetz L, D'Antonio M, Barry N, Sigurdardottir A, Bertolotti A. Preventing proteostasis diseases by selective inhibition of a phosphatase regulatory subunit. Science. 2015; 348:239–242. [PubMed: 25859045]

Deshaies RJ, Joazeiro CA. RING domain E3 ubiquitin ligases. Annu Rev Biochem. 2009; 78:399–434. [PubMed: 19489725]

Ellis RJ, Minton AP. Protein aggregation in crowded environments. Biol Chem. 2006; 387:485–497. [PubMed: 16740119]

Emmerich CH, Bakshi S, Kelsall IR, Ortiz-Guerrero J, Shpiro N, Cohen P. Lys63/Met1-hybrid ubiquitin chains are commonly formed during the activation of innate immune signalling. Biochem Biophys Res Commun. 2016

Emmerich CH, Ordureau A, Strickson S, Arthur JS, Pedrioli PG, Komander D, Cohen P. Activation of the canonical IKK complex by K63/M1-linked hybrid ubiquitin chains. Proceedings of the National Academy of Sciences of the United States of America. 2013; 110:15247–15252. [PubMed: 23986494]

Gardner RG, Nelson ZW, Gottschling DE. Degradation-mediated protein quality control in the nucleus. Cell. 2005; 120:803–815. [PubMed: 15797381]

Genetic Modifiers of Huntington's Disease, C. Identification of Genetic Factors that Modify Clinical Onset of Huntington's Disease. Cell. 2015; 162:516–526. [PubMed: 26232222]

Gidalevitz T, Ben-Zvi A, Ho KH, Brignull HR, Morimoto RI. Progressive disruption of cellular protein folding in models of polyglutamine diseases. Science. 2006; 311:1471–1474. [PubMed: 16469881]

Harper JW, Bennett EJ. Proteome complexity and the forces that drive proteome imbalance. Nature. 2016; 537:328–338. [PubMed: 27629639]

Hartl FU, Bracher A, Hayer-Hartl M. Molecular chaperones in protein folding and proteostasis. Nature. 2011; 475:324–332. [PubMed: 21776078]

Hessa T, Sharma A, Mariappan M, Eshleman HD, Gutierrez E, Hegde RS. Protein targeting and degradation are coupled for elimination of mislocalized proteins. Nature. 2011; 475:394–397. [PubMed: 21743475]

Hipp MS, Park SH, Hartl FU. Proteostasis impairment in protein-misfolding and -aggregation diseases. Trends Cell Biol. 2014; 24:506–514. [PubMed: 24946960]

Husnjak K, Dikic I. Ubiquitin-binding proteins: decoders of ubiquitin-mediated cellular functions. Annu Rev Biochem. 2012; 81:291–322. [PubMed: 22482907]

Huttlin EL, Ting L, Bruckner RJ, Gebreab F, Gygi MP, Szpyt J, Tam S, Zarraga G, Colby G, Baltier K, et al. The BioPlex Network: A Systematic Exploration of the Human Interactome. Cell. 2015; 162:425–440. [PubMed: 26186194]

Jin L, Williamson A, Banerjee S, Philipp I, Rape M. Mechanism of ubiquitin-chain formation by the human anaphase-promoting complex. Cell. 2008; 133:653–665. [PubMed: 18485873]

Juszkiewicz S, Hegde RS. Initiation of Quality Control during Poly(A) Translation Requires Site-Specific Ribosome Ubiquitination. Mol Cell. 2017; 65:743–750. e744. [PubMed: 28065601]

Kamadurai HB, Souphron J, Scott DC, Duda DM, Miller DJ, Stringer D, Piper RC, Schulman BA. Insights into ubiquitin transfer cascades from a structure of a UbcH5B approximately ubiquitin-HECT(NEDD4L) complex. Mol Cell. 2009; 36:1095–1102. [PubMed: 20064473]

Kelly A, Wickliffe KE, Song L, Fedrigo I, Rape M. Ubiquitin chain elongation requires e3-dependent tracking of the emerging conjugate. Mol Cell. 2014; 56:232–245. [PubMed: 25306918]

Kim HC, Huibregtse JM. Polyubiquitination by HECT E3s and the determinants of chain type specificity. Mol Cell Biol. 2009; 29:3307–3318. [PubMed: 19364824]

Kim HT, Kim KP, Lledias F, Kisselev AF, Scaglione KM, Skowyra D, Gygi SP, Goldberg AL. Certain pairs of ubiquitin-conjugating enzymes (E2s) and ubiquitin-protein ligases (E3s) synthesize nondegradable forked ubiquitin chains containing all possible isopeptide linkages. J Biol Chem. 2007; 282:17375–17386. [PubMed: 17426036]

Kirkpatrick DS, Hathaway NA, Hanna J, Elsasser S, Rush J, Finley D, King RW, Gygi SP. Quantitative analysis of in vitro ubiquitinated cyclin B1 reveals complex chain topology. Nat Cell Biol. 2006; 8:700–710. [PubMed: 16799550]

Koegl M, Hoppe T, Schlenker S, Ulrich HD, Mayer TU, Jentsch S. A novel ubiquitination factor, E4, is involved in multiubiquitin chain assembly. Cell. 1999; 96:635–644. [PubMed: 10089879]

Komander D, Rape M. The ubiquitin code. Annual review of biochemistry. 2012; 81:203–229.

Kristariyanto YA, Abdul Rehman SA, Campbell DG, Morrice NA, Johnson C, Toth R, Kulathu Y. K29-selective ubiquitin binding domain reveals structural basis of specificity and heterotypic nature of k29 polyubiquitin. Mol Cell. 2015; 58:83–94. [PubMed: 25752573]

Langfelder P, Cantle JP, Chatzopoulou D, Wang N, Gao F, Al-Ramahi I, Lu XH, Ramos EM, El-Zein K, Zhao Y, et al. Integrated genomics and proteomics define huntingtin CAG length-dependent networks in mice. Nat Neurosci. 2016; 19:623–633. [PubMed: 26900923]

Lipkowitz S, Weissman AM. RINGs of good and evil: RING finger ubiquitin ligases at the crossroads of tumour suppression and oncogenesis. Nat Rev Cancer. 2011; 11:629–643. [PubMed: 21863050]

Liu C, Liu W, Ye Y, LI W. Ufd2p synthesizes branched ubiquitin chains to promote the degradation of substrates modified with atypical chains. Nat Commun. 2017; 8:14274. [PubMed: 28165462]

Matsumoto ML, Dong KC, Yu C, Phu L, Gao X, Hannoush RN, Hymowitz SG, Kirkpatrick DS, Dixit VM, Kelley RF. Engineering and structural characterization of a linear polyubiquitin-specific antibody. Journal of molecular biology. 2012; 418:134–144. [PubMed: 22227388]

Matsumoto ML, Wickliffe KE, Dong KC, Yu C, Bosanac I, Bustos D, Phu L, Kirkpatrick DS, Hymowitz SG, Rape M, et al. K11-linked polyubiquitination in cell cycle control revealed by a K11 linkage-specific antibody. Mol Cell. 2010; 39:477–484. [PubMed: 20655260]

Meacham GC, Patterson C, Zhang W, Younger JM, Cyr DM. The Hsc70 co-chaperone CHIP targets immature CFTR for proteasomal degradation. Nat Cell Biol. 2001; 3:100–105. [PubMed: 11146634]

Merchant AM, Zhu Z, Yuan JQ, Goddard A, Adams CW, Presta LG, Carter P. An efficient route to human bispecific IgG. Nat Biotechnol. 1998; 16:677–681. [PubMed: 9661204]

Meyer HJ, Rape M. Enhanced protein degradation by branched ubiquitin chains. Cell. 2014; 157:910–921. [PubMed: 24813613]

Miller J, Arrasate M, Brooks E, Libeu CP, Legleiter J, Hatters D, Curtis J, Cheung K, Krishnan P, Mitra S, et al. Identifying polyglutamine protein species in situ that best predict neurodegeneration. Nat Chem Biol. 2011; 7:925–934. [PubMed: 22037470]

Moir D, Stewart SE, Osmond BC, Botstein D. Cold-sensitive cell-division-cycle mutants of yeast: isolation, properties, and pseudoreversion studies. Genetics. 1982; 100:547–563. [PubMed: 6749598]

Newton K, Matsumoto ML, Wertz IE, Kirkpatrick DS, Lill JR, Tan J, Dugger D, Gordon N, Sidhu SS, Fellouse FA, et al. Ubiquitin chain editing revealed by polyubiquitin linkage-specific antibodies. Cell. 2008; 134:668–678. [PubMed: 18724939]

Ohtake F, Saeki Y, Ishido S, Kanno J, Tanaka K. The K48-K63 Branched Ubiquitin Chain Regulates NF-kappaB Signaling. Mol Cell. 2016; 64:251–266. [PubMed: 27746020]

Plechanovova A, Jaffray EG, Tatham MH, Naismith JH, Hay RT. Structure of a RING E3 ligase and ubiquitin-loaded E2 primed for catalysis. Nature. 2012; 489:115–120. [PubMed: 22842904]

Rape M, Kirschner MW. Autonomous regulation of the anaphase-promoting complex couples mitosis to S-phase entry. Nature. 2004; 432:588–595. [PubMed: 15558010]

Ravid T, Hochstrasser M. Diversity of degradation signals in the ubiquitin-proteasome system. Nat Rev Mol Cell Biol. 2008; 9:679–690. [PubMed: 18698327]

Reddy SK, Rape M, Margansky WA, Kirschner MW. Ubiquitination by the anaphase-promoting complex drives spindle checkpoint inactivation. Nature. 2007; 446:921–925. [PubMed: 17443186]

Rodrigo-Brenni MC, Gutierrez E, Hegde RS. Cytosolic quality control of mislocalized proteins requires RNF126 recruitment to Bag6. Mol Cell. 2014; 55:227–237. [PubMed: 24981174]

Rotin D, Kumar S. Physiological functions of the HECT family of ubiquitin ligases. Nat Rev Mol Cell Biol. 2009; 10:398–409. [PubMed: 19436320]

Saunders DN, Hird SL, Withington SL, Dunwoodie SL, Henderson MJ, Biben C, Sutherland RL, Ormandy CJ, Watts CK. Edd, the murine hyperplastic disc gene, is essential for yolk sac vascularization and chorioallantoic fusion. Mol Cell Biol. 2004; 24:7225–7234. [PubMed: 15282321]

Scaglione KM, Zavodszky E, Todi SV, Patury S, Xu P, Rodriguez-Lebron E, Fischer S, Konen J, Djarmati A, Peng J, et al. Ube2w and Ataxin-3 Coordinately Regulate the Ubiquitin Ligase CHIP. Mol Cell. 2011; 43:599–612. [PubMed: 21855799]

Scialpi F, Mellis D, Ditzel M. EDD, a ubiquitin-protein ligase of the N-end rule pathway, associates with spindle assembly checkpoint components and regulates the mitotic response to nocodazole. J Biol Chem. 2015; 290:12585–12594. [PubMed: 25833949]

Sha Z, Brill LM, Cabrera R, Kleifeld O, Scheliga JS, Glickman MH, Chang EC, Wolf DA. The eIF3 interactome reveals the translasome, a supercomplex linking protein synthesis and degradation machineries. Mol Cell. 2009; 36:141–152. [PubMed: 19818717]

Shao S, Brown A, Santhanam B, Hegde RS. Structure and assembly pathway of the ribosome quality control complex. Mol Cell. 2015; 57:433–444. [PubMed: 25578875]

Shemorry A, Hwang CS, Varshavsky A. Control of protein quality and stoichiometries by N-terminal acetylation and the N-end rule pathway. Mol Cell. 2013; 50:540–551. [PubMed: 23603116]

Sivakumar S, Gorbsky GJ. Spatiotemporal regulation of the anaphase-promoting complex in mitosis. Nat Rev Mol Cell Biol. 2015; 16:82–94. [PubMed: 25604195]

Skaar JR, Pagan JK, Pagano M. Mechanisms and function of substrate recruitment by F-box proteins. Nat Rev Mol Cell Biol. 2013; 14:369–381. [PubMed: 23657496]

Spence J, Sadis S, Haas AL, Finley D. A ubiquitin mutant with specific defects in DNA repair and multiubiquitination. Mol Cell Biol. 1995; 15:1265–1273. [PubMed: 7862120]

Sundaramoorthy E, Leonard M, Mak R, Liao J, Fulzele A, Bennett EJ. ZNF598 and RACK1 Regulate Mammalian Ribosome-Associated Quality Control Function by Mediating Regulatory 40S Ribosomal Ubiquitylation. Mol Cell. 2017; 65:751–760. e754. [PubMed: 28132843]

Sung MK, Porras-Yakushi TR, Reitsma JM, Huber FM, Sweredoski MJ, Hoelz A, Hess S, Deshaies RJ. A conserved quality-control pathway that mediates degradation of unassembled ribosomal proteins. Elife. 2016; 5

Tasaki T, Kim ST, Zakrzewska A, Lee BE, Kang MJ, Yoo YD, Cha-Molstad HJ, Hwang J, Soung NK, Sung KS, et al. UBR box N-recognin-4 (UBR4), an N-recognin of the N-end rule pathway, and its role in yolk sac vascular development and autophagy. Proc Natl Acad Sci U S A. 2013; 110:3800–3805. [PubMed: 23431188]

Tokunaga F, Sakata S, Saeki Y, Satomi Y, Kirisako T, Kamei K, Nakagawa T, Kato M, Murata S, Yamaoka S, et al. Involvement of linear polyubiquitylation of NEMO in NF-kappaB activation. Nat Cell Biol. 2009; 11:123–132. [PubMed: 19136968]

Turner GC, Varshavsky A. Detecting and measuring cotranslational protein degradation in vivo. Science. 2000; 289:2117–2120. [PubMed: 11000112]

Verma R, Oania RS, Kolawa NJ, Deshaies RJ. Cdc48/p97 promotes degradation of aberrant nascent polypeptides bound to the ribosome. Elife. 2013; 2:e00308. [PubMed: 23358411]

Wang C, Deng L, Hong M, Akkaraju GR, Inoue J, Chen ZJ. TAK1 is a ubiquitin-dependent kinase of MKK and IKK. Nature. 2001; 412:346–351. [PubMed: 11460167]

Wang F, Canadeo LA, Huibregtse JM. Ubiquitination of newly synthesized proteins at the ribosome. Biochimie. 2015a; 114:127–133. [PubMed: 25701549]

Wang F, Durfee LA, Huibregtse JM. A cotranslational ubiquitination pathway for quality control of misfolded proteins. Mol Cell. 2013; 50:368–378. [PubMed: 23583076]

Wang T, Birsoy K, Hughes NW, Krupczak KM, Post Y, Wei JJ, Lander ES, Sabatini DM. Identification and characterization of essential genes in the human genome. Science. 2015b; 350:1096–1101. [PubMed: 26472758]

Weishaupt JH, Hyman T, Dikic I. Common Molecular Pathways in Amyotrophic Lateral Sclerosis and Frontotemporal Dementia. Trends in molecular medicine. 2016; 22:769–783. [PubMed: 27498188]

Wertz IE, Newton K, Seshasayee D, Kusam S, Lam C, Zhang J, Popovych N, Helgason E, Schoeffler A, Jeet S, et al. Phosphorylation and linear ubiquitin direct A20 inhibition of inflammation. Nature. 2015; 528:370–375. [PubMed: 26649818]

Wickliffe KE, Lorenz S, Wemmer DE, Kuriyan J, Rape M. The mechanism of linkage-specific ubiquitin chain elongation by a single-subunit e2. Cell. 2011; 144:769–781. [PubMed: 21376237]

Williamson A, Wickliffe KE, Mellone BG, Song L, Karpen GH, Rape M. Identification of a physiological E2 module for the human anaphase-promoting complex. Proc Natl Acad Sci U S A. 2009; 106:18213–18218. [PubMed: 19822757]

Xu P, Duong DM, Seyfried NT, Cheng D, Xie Y, Robert J, Rush J, Hochstrasser M, Finley D, Peng J. Quantitative proteomics reveals the function of unconventional ubiquitin chains in proteasomal degradation. Cell. 2009; 137:133–145. [PubMed: 19345192]

Xu Y, Anderson DE, Ye Y. The HECT domain ubiquitin ligase HUWE1 targets unassembled soluble proteins for degradation. Cell Discov. 2016; 2:16040. [PubMed: 27867533]

Yamaguchi M, VanderLinden R, Weissmann F, Qiao R, Dube P, Brown NG, Haselbach D, Zhang W, Sidhu SS, Peters JM, et al. Cryo-EM of Mitotic Checkpoint Complex-Bound APC/C Reveals Reciprocal and Conformational Regulation of Ubiquitin Ligation. Mol Cell. 2016; 63:593–607. [PubMed: 27522463]

Yau R, Rape M. The increasing complexity of the ubiquitin code. Nat Cell Biol. 2016; 18:579–586. [PubMed: 27230526]

Younger JM, Chen L, Ren HY, Rosser MF, Turnbull EL, Fan CY, Patterson C, Cyr DM. Sequential quality-control checkpoints triage misfolded cystic fibrosis transmembrane conductance regulator. Cell. 2006; 126:571–582. [PubMed: 16901789]

Highlights

- K11/K48-bispecific antibodies detect endogenous K11/K48-linked ubiquitin chains.
- K11/K48-branched chains modify mitotic regulators and misfolded nascent proteins.
- K11/K48-dependent proteasomal degradation prevents protein aggregation.
- Mutations in K11/K48-specific enzymes are found in neurodegenerative diseases.

Bispecific antibodies reveal the presence and function of heterotypic ubiquitin chains containing K11 and K48 linkages in cell cycle regulation and protein quality control.

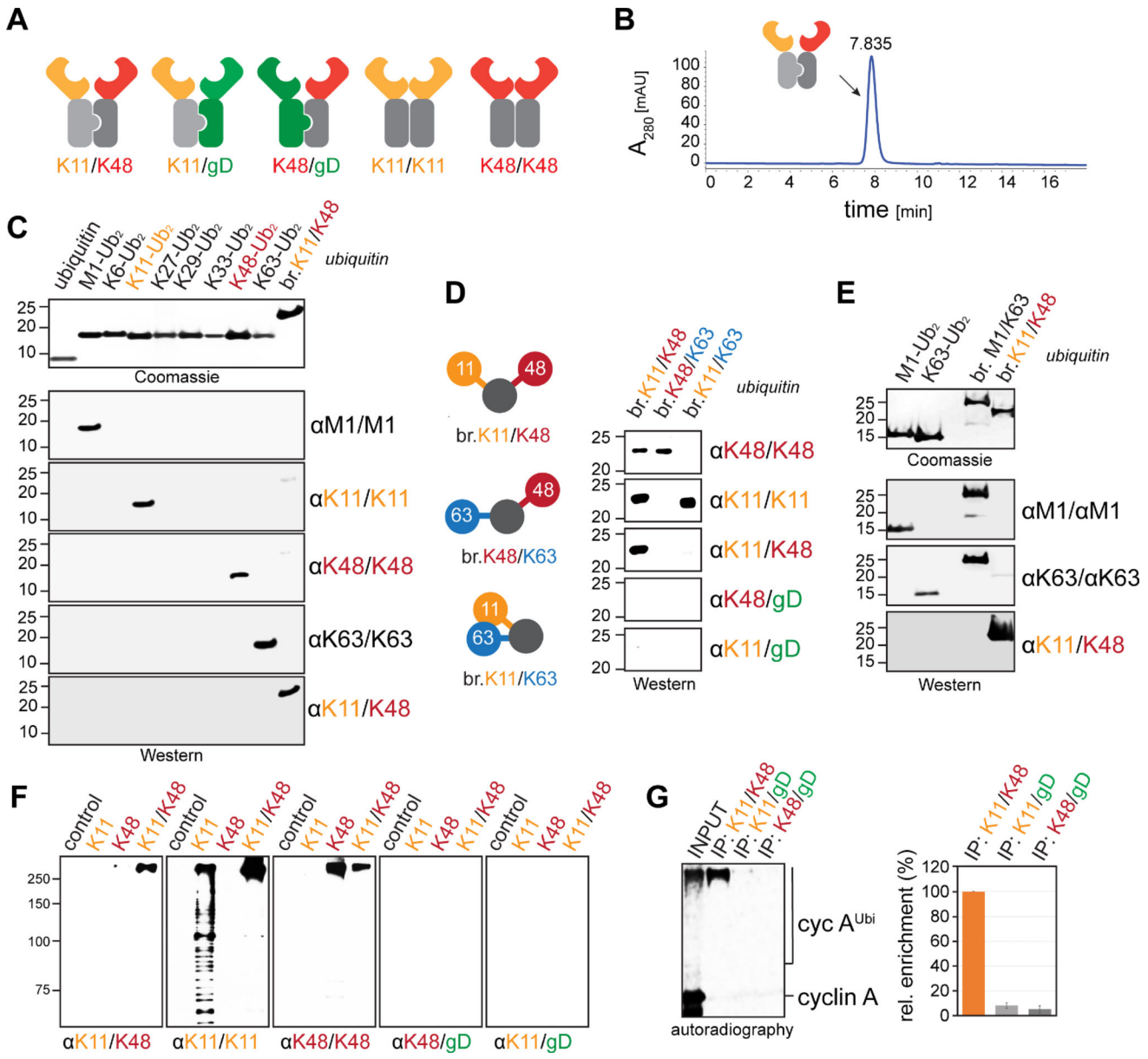

Figure 1. A bispecific antibody specifically detects K11/K48-linked heterotypic ubiquitin chains

A. Overview of bispecific antibodies produced in this study, as well as established K11- and K48-monospecific antibodies (Matsumoto et al., 2010; Newton et al., 2008). **B.** Final size exclusion chromatography of K11/K48-bispecific antibody purification. **C.** The K11/K48-bispecific antibody detects K11/K48-branched ubiquitin trimers. Equal levels of monomeric ubiquitin, all possible ubiquitin dimers, and K11/K48-branched ubiquitin trimers were analyzed by Coomassie gel electrophoresis or Western blots using the indicated antibodies. **D.** The K11/K48-bispecific antibody detects K11/K48-, but not K11/K63- or K48/K63-branches. Equal concentrations of branched ubiquitin trimers were analyzed by Western blotting using the indicated antibodies at identical antibody concentrations and exposure times. **E.** The K11/K48- bispecific antibody detects K11/K48-, but not M1/K63-branched ubiquitin. Recombinant ubiquitin trimers were analyzed as described above. **F.** The K11/

K48-bispecific antibody can discriminate high molecular weight ubiquitin chains. An engineered ubiquitin ligation system (Meyer and Rape, 2014) using the E3 APC/C, the E2 enzymes UBE2S and/or UBE2G2^{CTP}, and ubiquitin, was used to generate K11/K48-branched chains and homotypic K11- or K48-linked chains. Chain formation was analyzed by using the K11/K48-bispecific antibody or established monospecific antibodies that recognize the K11- or K48-linkage, respectively. Western blots were analyzed at identical antibody concentrations and exposure times (i.e. explaining the lack of signal with control antibodies). **G.** The K11/K48-bispecific antibody allows for purification of K11/K48-branched chains by immunoprecipitation. K11/K48-branched ubiquitin chains were assembled on the ^{35}S-labeled APC/C-substrate cyclin A as described (Meyer and Rape, 2014), and conjugates were affinity-purified using identical concentrations of K11/K48-, K11/gD-, or K48/gD-antibodies. The purified radioactivity was quantified after autoradiography; quantification is shown of three independent experiments; (n=3; SEM).

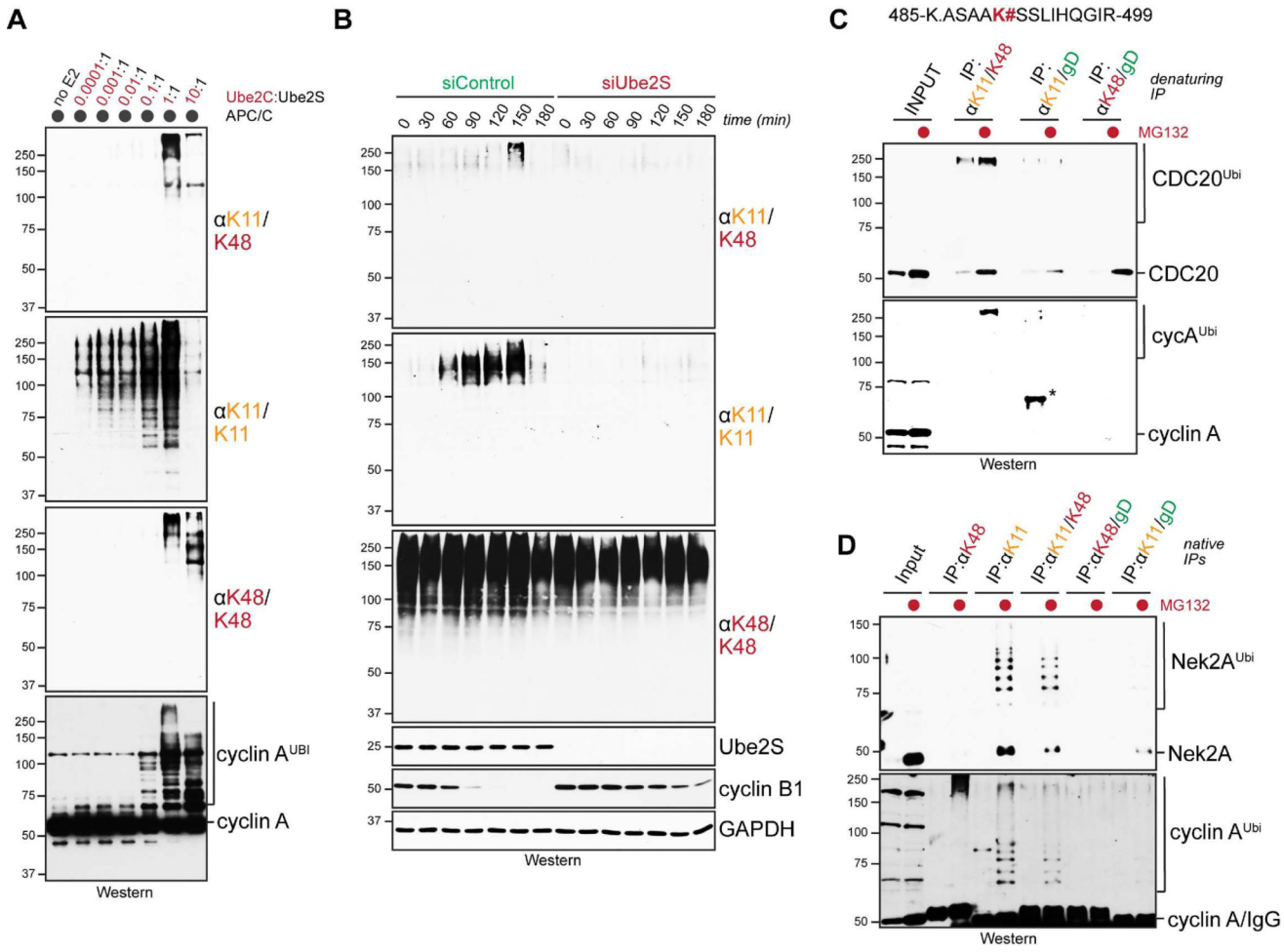

Figure 2. The APC/C assembles heterotypic K11/K48-linked chains

A. The APC/C produces K11/K48-linked ubiquitin chains *in vitro*. APC/C purified from human mitotic cells was incubated with increasing concentrations of the initiating E2 UBE2C, constant levels of the branching E2 UBE2S, and the substrate cyclin A. Ubiquitylation of cyclin A was assessed by Western blotting using the indicated antibodies. **B.** K11/K48-linked chains accumulate during mitosis. HeLa cells were synchronized in prometaphase, released into cell division, and subjected to protein expression analysis at the indicated time points. Cells were either transfected with control siRNAs or validated siRNAs targeting UBE2S (Kelly et al., 2014). **C.** CDC20 and cyclin A are modified with K11/K48-branched chains in cells. *Above:* CDC20 peptides ubiquitylated at Lys490 were only detected in K11/K48-bispecific, but not in K11/gD- or K48/gD-control affinity-purifications. Other ubiquitylation sites were not detected on CDC20. *Lower panel:* Affinity-purifications of ubiquitin chains from mitotic lysates were performed with the indicated antibodies under denaturing conditions. Co-purifying endogenous CDC20 or cyclin A was detected by a specific antibody. The asterisk marks a non-specific band caused by serendipitous antibody dissociation during elution. **D.** Endogenous NEK2A and cyclin A are likely modified with K11/K48-linked ubiquitin chains. Ubiquitin conjugates of different topologies were affinity-purified from mitotic HeLa cells grown either in the presence or absence of proteasome

inhibitors and analyzed by Western blotting using specific antibodies. The inability of the K48-specific antibody to purify NEK2A is likely caused by few K48-linkages that are buried in the branched ubiquitin conjugate (Meyer and Rape, 2014). Endogenous cyclin A is modified with either K11/K48-linked ubiquitin chains or with distinct conjugates containing K48-, but less so K11-linkages.

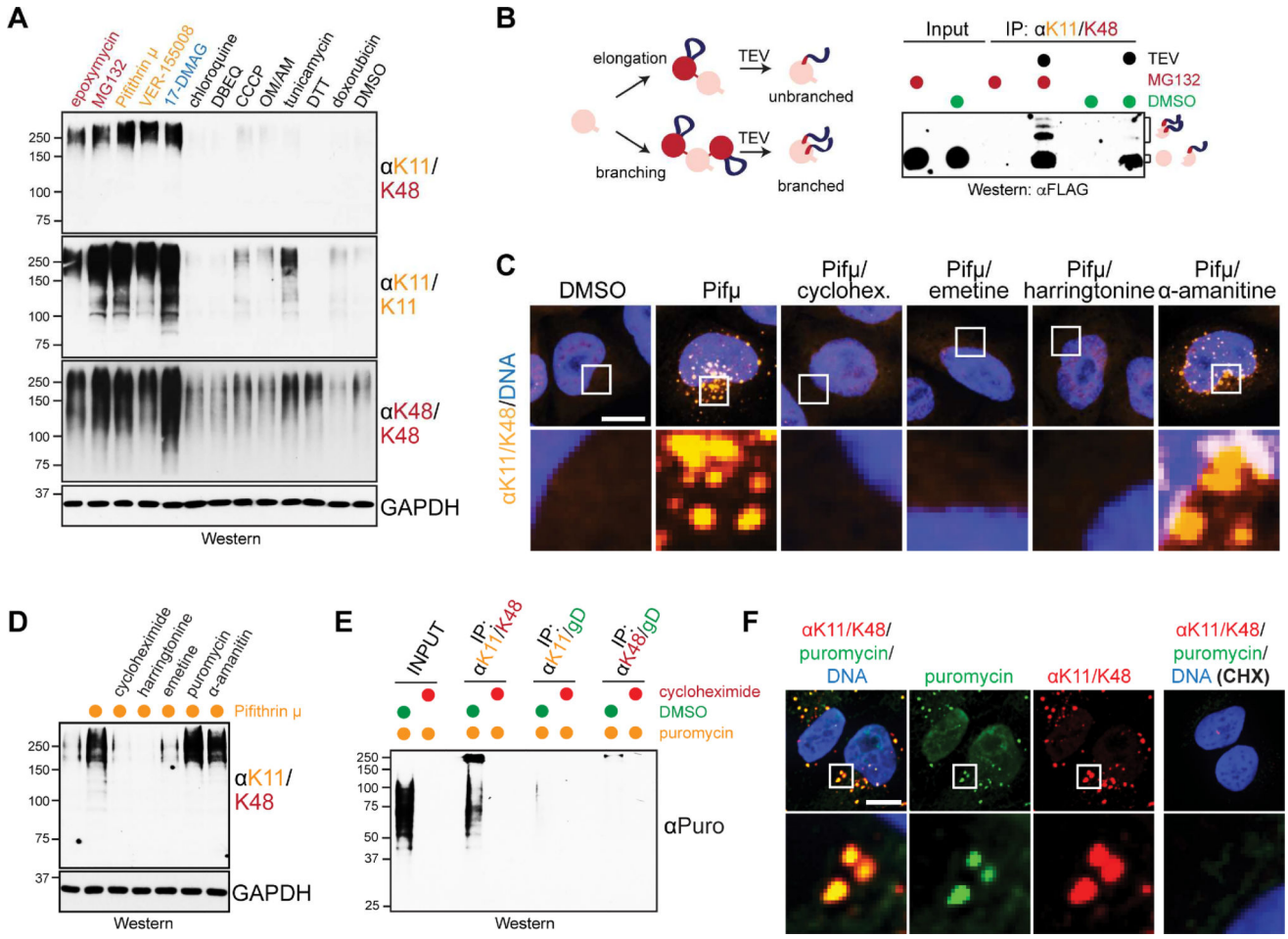

Figure 3. Cells respond to proteotoxic stress by assembling K11/K48-branched chains

A. 293T cells were treated with proteasome- (red), HSP70- (yellow), HSP90-inhibitors (blue), or other stressors, and formation of ubiquitin chains with the indicated topologies was monitored by Western blotting using specific antibodies. **B.** Accumulation of misfolded proteins results in formation of K11/K48-branched chains. 293T cells expressing ubiquitin$^{TEV/FLAG}$ were grown in the presence of MG132 as indicated. K11/K48-linked chains were affinity-purified using the K11/K48-bispecific antibody and subjected to TEV cleavage. As each attached ubiquitin$^{TEV/FLAG}$ leaves a ~2kD “stamp”, branched ubiquitin molecules with two or more stamps can be detected by αFLAG Western blotting (Meyer and Rape, 2014). Only the relevant MW region of the αFLAG Western blot is shown. **C.** Aggregating newly synthesized proteins are strongly labeled with K11/K48-linked chains. Cells were treated with either DMSO or the HSP70 inhibitor pifithrin μ, and then stained for K11/K48-linked chains by using fluorescently labeled K11/K48-bispecific antibodies (yellow). DNA was stained with Hoechst (blue). Inhibition of mRNA translation (cycloheximide, emetine, harringtonine), but not inhibition of transcription (α-amanitine), prevented formation of K11/K48-positive aggregates. **D.** Production of K11/K48-linked chains in cells experiencing proteotoxic stress relies on new protein synthesis. 293T cells were treated with the HSP70-inhibitor pifithrin μ, and various inhibitors of mRNA translation or transcription, as described above. K11/K48-linked chains were detected by

Western blotting using bispecific antibodies. **E.** Nascent, misfolded proteins are decorated with K11/K48-linked chains. Ubiquitin conjugates from puromycin-treated 293T cells were purified under denaturing conditions using the indicated antibodies, and modified puromycylated proteins were detected with an antibody against puromycin. **F.** Puromycylated proteins accumulate in K11/K48-positive aggregates. HeLa cells were treated with puromycin for 2h and analyzed by immunofluorescence microscopy against puromycin (green), K11/K48-linked chains (red), and DNA (blue). The right panel depicts a merged image of the same experiment performed in the presence of cycloheximide.

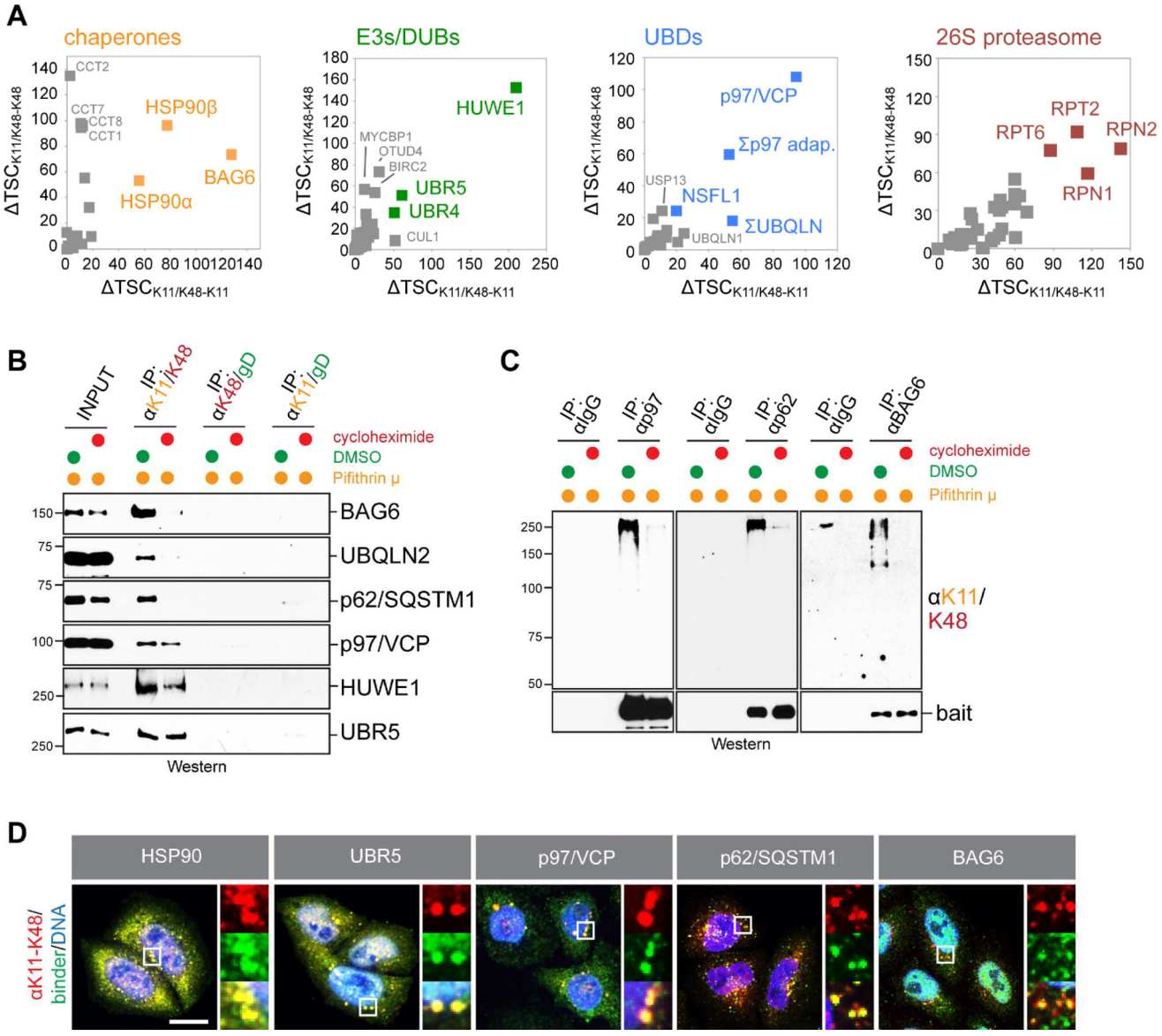

Figure 4. Identification of enzymes and effectors of K11/K48-specific quality control

A. Ubiquitin chains were purified from puromycin-treated cells using K11/K48-bispecific, K11/gD-, or K48/gD-control antibodies. 5 biological and 1 technical replicates were used for label-free quantitative mass spectrometry to identify proteins enriched in K11/K48-bispecific purifications (colored proteins were significantly enriched compared to control purifications; $p<0.01$). Axis show enrichment compared to K11- ($TSC_{K11/K48}$-TSC_{K11}) or K48-linkages ($TSC_{K11/K48}$-TSC_{K48}), based on average TSC/experiment. **B.** Ubiquitin chains of the indicated topology were affinity- purified from 293T cells treated with pifithrin μ and analyzed for co-purifying proteins using Western blotting and specific antibodies. Cycloheximide was added as noted to prevent the production of newly synthesized proteins. **C.** p97, BAG6, and p62/SQSTM1 bind K11/K48-linked chains in an mRNA-translation dependent manner. Endogenous p97, BAG6, or p62 were affinity-purified from cells treated with the HSP70-inhibitor pifithrin μ. When indicated, cells were also exposed to

cycloheximide. Bound K11/K48-linked ubiquitin chains were detected by Western blotting using the K11/K48-bispecific antibody. **D.** Enzymes and effectors of K11/K48- specific quality control co-localize with K11/K48-positive protein aggregates. HeLa cells treated with either proteasome or HSP70-inhibitors were stained for K11/K48-linked chains (red); binding proteins identified by mass spectrometry (green), and DNA (blue).

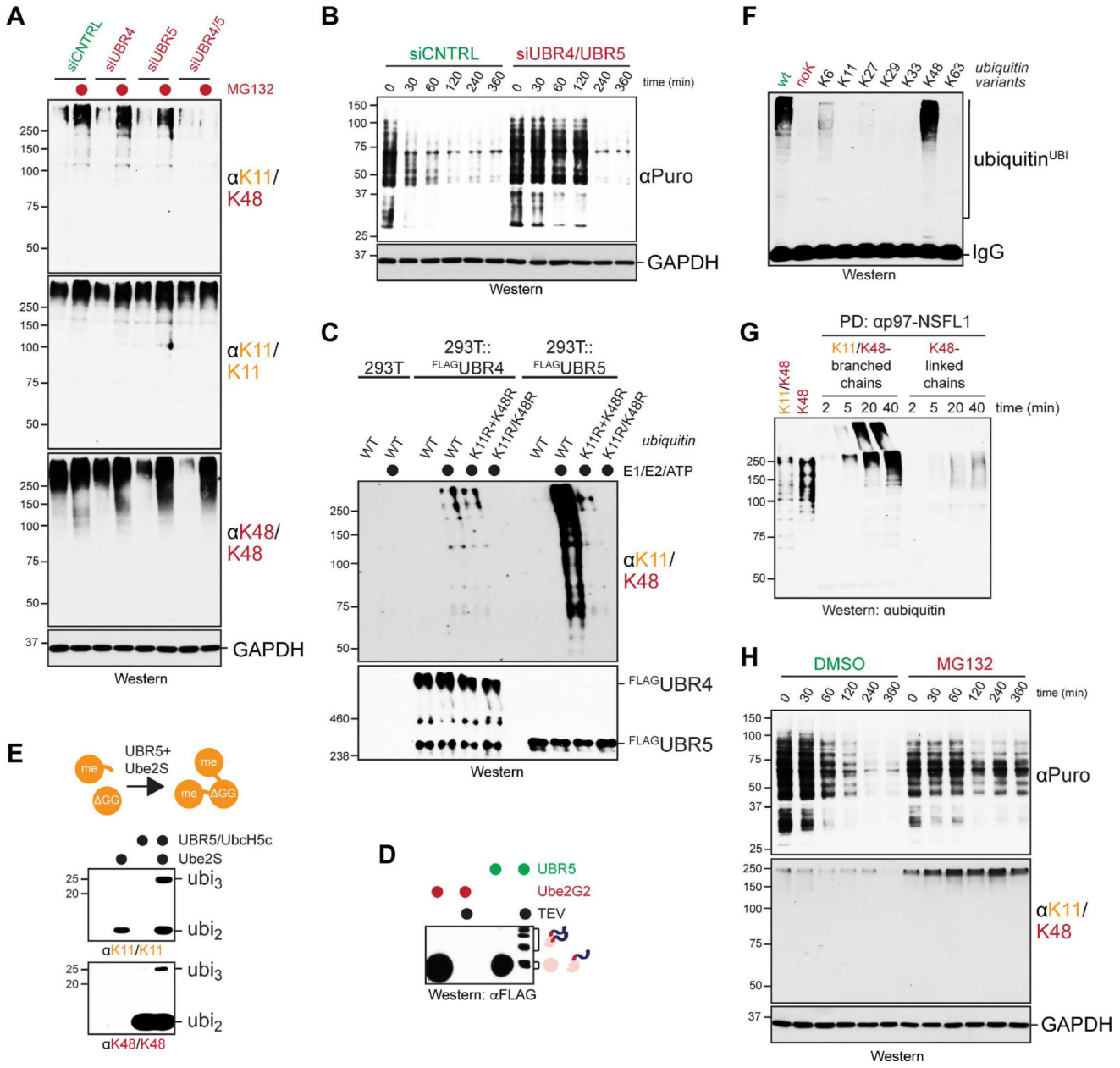

Figure 5. Functional analysis of components of K11/K48-specific quality control

A. UBR4 and UBR5 assemble most K11/K48-linked chains during quality control. 293T cells were co- depleted of UBR4 and UBR5, treated with MG132, and analyzed for ubiquitin chains of different topologies using Western blotting. **B.** UBR4 and UBR5 target puromycylated proteins for degradation. 293T cells were co-depleted of UBR4 and UBR5, treated with puromycin, and the stability of puromycylated proteins was determined by cycloheximide chase and Western blotting. **C.** UBR4 and UBR5 complexes synthesize K11/K48-linked chains *in vitro*. Endogenous ^{FLAG}UBR4 and ^{FLAG}UBR5 were affinity-purified from CRISPR/Cas9-edited 293T cells, incubated with E1, the E2 UBE2D3, and ATP (as indicated). Reactions were supplemented with wild-type ubiquitin (WT); a mixture of ubiquitin^{K11R} and ubiquitin^{K48R} (K11R+K48R) or double mutant ubiquitin$^{K11R/K48R}$

(K11R/K48R). Reactions were analyzed for K11/K48-linked chains and the respective E3 enzymes by Western blotting. **D.** UBR5 assembles branched ubiquitin chains. Affinity-purified ^{FLAG}UBR5 were incubated with E1, UBE2D3, and ubiquitin$^{FLAG/TEV}$. Conjugates were treated with TEV-protease as indicated and analyzed by αFLAG immunoblotting. The presence of two or more FLAG-positive stamps indicates branching. As control, ubiquitylation reactions were performed with UBE2G2/gp78, which only assemble homotypic K48-linked chains. **E.** UBR5 produces branched ubiquitin trimers. UBR5 and the K11-specific UBE2S were incubated with ubiquitin$^{\Delta GG}$ (a mutant that can be modified, but not used as a modifier) and methyl-ubiquitin (which can be transferred to ubiquitin$^{\Delta GG}$, but not further modified), as indicated. Formation of K11- or K48-positive ubiquitin conjugates was analyzed by linkage-specific Western blotting. The presence of both UBE2S and UBR5 leads to formation of branched ubiquitin trimers. **F.** UBR5 strongly prefers K48-linkages. Endogenous UBR5 complexes were incubated with indicated single-Lys ubiquitin mutants and analyzed by αUbiquitin immunoblotting. **G.** K11/K48-branched ubiquitin chains produced by UBR5 show strongly increased affinity to the p97/VCP adaptor NSFL1/p47 than homotypic K48-linked chains. K11/K48-branched or K48-linked chains were assembled by UBR5 using wt-ubiquitin or ubiquitin^{K48} and incubated with immobilized p97-NSFL1 complexes. Binding reactions were stopped at the indicated times and analyzed by αUbiquitin immunoblotting. **H.** The proteasome targets puromycylated and K11/K48-labeled proteins for degradation. The stability of puromycylated proteins was analyzed in cells treated with DMSO or MG132, and puromycylated proteins or K11/K48-linked chains were detected by Western blotting using specific antibodies.

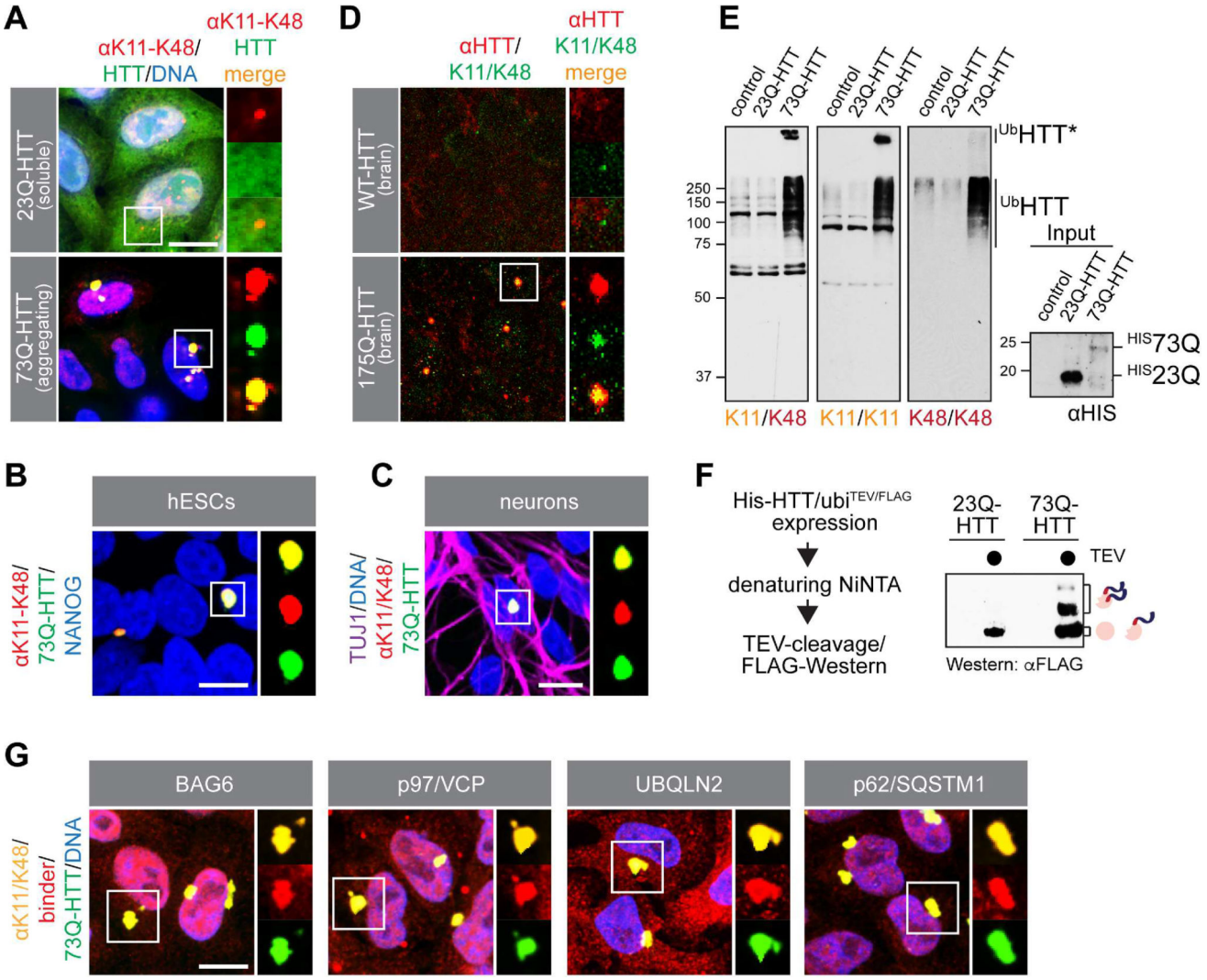

Figure 6. K11/K48-specific quality control targets pathological HTT variants

a. Expression of 73Q-HTT, but not benign 23Q-HTT, causes formation of K11/K48-positive aggregates. HeLa cell lines were generated that express, under an inducible promoter, constructs for exon 1 of 23Q- or 73Q-HTT fused to GFP. Following induction of HTT, cells were stained for K11/K48- linked chains (red), ^{GFP}HTT (green), or DNA (blue). The right panel shows the insert from top to bottom: K11/K48-linked chains, ^{GFP}HTT, and merge. **B.** 73Q-HTT aggregates are labeled with K11/K48-linked chains in untransformed human embryonic stem cells. Following induction of HTT in H1 hESCs, cells were stained for K11/K48-linked chains (red), ^{GFP}HTT (green), or the ESC marker Nanog (blue). **C.** 73Q-HTT aggregates are labeled with K11/K48-linked chains in differentiated neurons obtained from H1 hESCs by long-term neural conversion. Following induction of HTT in neurons, cells were stained for K11/K48-linked chains (red), ^{GFP}HTT (green), the neuronal marker Tuj1 (purple), and DNA (blue). **D.** 175Q-HTT aggregates are labeled with K11/K48-linked chains in brains of a mouse model of Huntington's Disease. Maximum projections of brain slices of wt- or 175Q-HTT expressing mice stained with antibodies against HTT (red) or K11/K48-linked chains (green). **E.** 73Q-HTT is modified with K11/K48-linked chains. Lysates of

HeLa cells expressing HIS_6-tagged exon 1 of 23Q- or 73Q-HTT were subjected to denaturing NiNTA-purification, and bound proteins were analyzed by Western blotting using linkage-specific ubiquitin antibodies. HTT* marks an aggregated, SDS-resistant species. The input is shown below. **F.** 73Q-HTT, but not 23Q-HTT, is modified with branched ubiquitin chains. HTT variants were purified under denaturing conditions, including removal of any remaining aggregates, from cells expressing $ubiquitin^{TEV/FLAG}$ using NiNTA agarose. Conjugates were treated on beads with TEV protease and analyzed for branching using αFLAG Western blotting. **G.** 73Q-HTT is recognized by effectors of K11/K48-specific quality control. Following induction of ^{GFP}73Q-HTT, HeLa cells were stained for 73Q-HTT (green), K11/K48- linked chains (yellow), BAG6, p97, UBQLN2, or p62 as indicated (red), and DNA (blue). The panel on the right of each microscopy picture shows independent channels for K11/K48-linked chains (yellow), ubiquitin-binder (red), and ^{GFP}HTT (green).

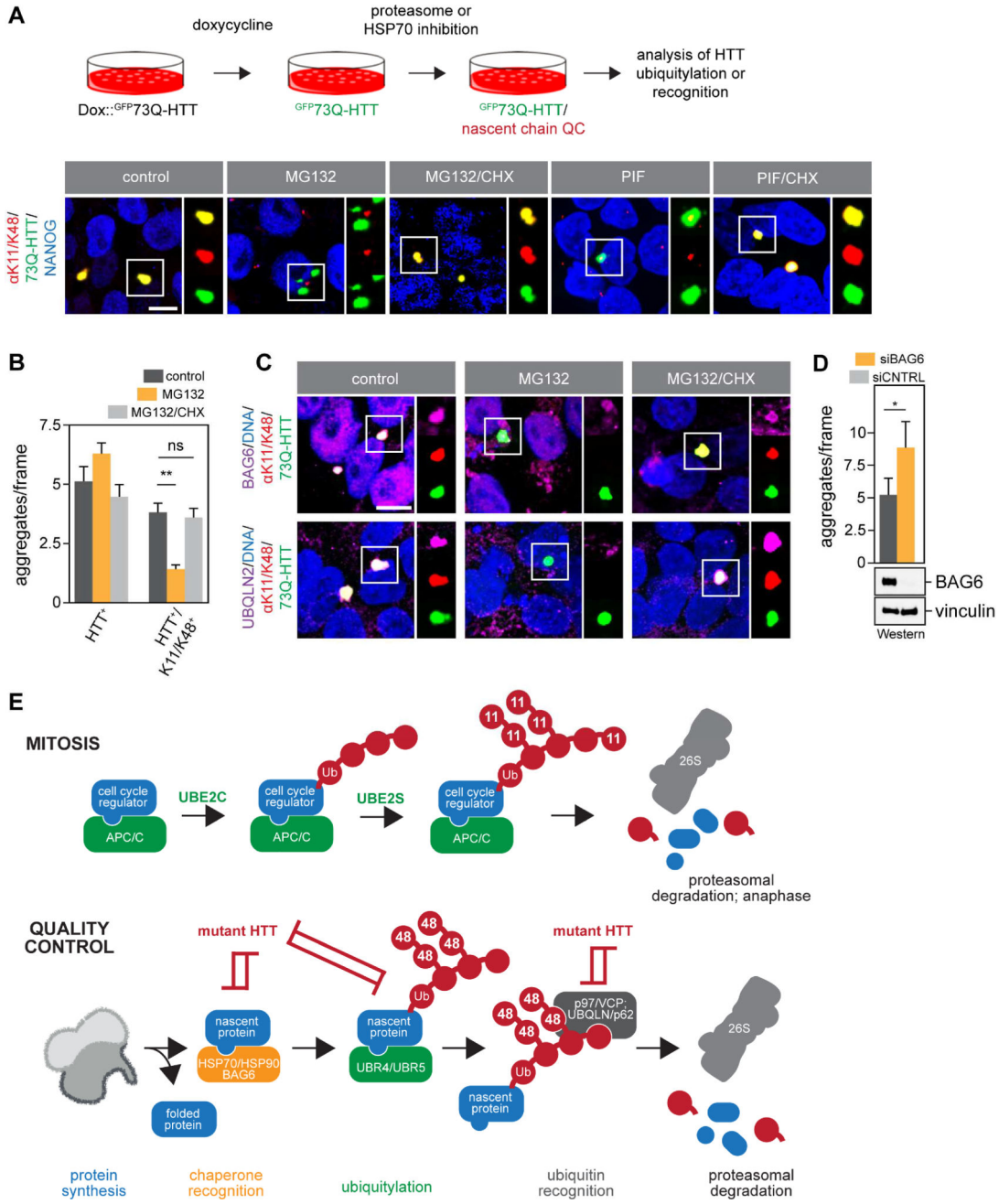

Figure 7. K11/K48-specific quality control has a limited capacity to handle pathological HTT and newly synthesized, misfolded proteins

A. 73Q-HTT and nascent proteins compete for access to the K11/K48-specific quality control machinery. Following expression of 73Q-HTT, human embryonic stem cells were treated for 4–6h with either DMSO (control), MG132 or pifithrin μ (PIF) to stabilize newly synthesized, misfolded proteins. As indicated, cycloheximide (CHX) was added to determine effects of new protein synthesis on proteasome- or HSP70- inhibited cells. Cells were stained for 73Q-HTT (green), K11/K48-linked chains (red) or the hESC marker Nanog (blue). The right panel shows following channels of the insert, from top to bottom: merge of K11/K48-linked chains and 73Q-HTT; K11/K48-linked chains; 73Q-HTT. **B.** Quantification

of K11/K48-positive HTT aggregates in hESCs treated with DMSO (control), MG132, or MG132 and cycloheximide (MG132/CHX). Only complete loss of K11/K48-staining was counted (i.e. reduction in staining still counted as a positive aggregate). (HTT^+: all HTT aggregates; HTT^+/$K11/K48^+$: K11/K48-positive HTT aggregates). Average of three biological replicates -/+ s.e.m. are depicted and significance was determined by an unpaired t-test (** $p<0.005$). **C.** 73Q-HTT and nascent proteins compete for effectors of K11/K48-specific quality control. Following induction of 73Q-HTT expression, human embryonic stem cells were treated with either DMSO (control), MG132 or MG132/cycloheximide (CHX). Cells were stained for 73Q-HTT (green), K11/K48-linked chains (red), the K11/K48-effectors BAG6 or UBQLN2 (purple) and DNA (blue). The right panel shows the following channels of the insert, from top to bottom: BAG6 or UBQLN2 (purple); K11/K48-linked chains (red); 73Q-HTT (green). **D.** Depletion of BAG6 results in more HTT aggregates. hESCs were depleted of BAG6 using siRNAs and treated with doxycycline to induce expression of 73Q-HTT. The number of 73Q- HTT aggregates was determined by random image acquisition and analysis using Image J. Average of four biological replicates -/+ s.e.m. are depicted and significance was determined by a paired t-test. (*: $p<0.05$). **E.** *Upper panel:* model of K11/K48-branched chain formation during mitosis. The APC/C and its specific E2 enzymes UBE2C and UBE2S produce K11/K48-branched conjugates characterized by multiple blocks of K11-linked chains. As shown before (Meyer and Rape, 2014), such chains effectively trigger proteasomal degradation of cell cycle regulators. *Lower panel:* model of K11/K48-specific quality control. Newly synthesized, misfolded proteins coming are initially recognized by chaperones, including HSP90 and BAG6. If their folding fails on multiple attempts, such misfolded proteins are recognized by the E3 ligases UBR4 and UBR5, which modify their targets with K11/K48-branched chains. K11/K48-ubiquitylated substrates are recognized by the ubiquitin-selective segregase p97/VCP and proteasome shuttles of the UBQLN family. This results in their removal from protein complexes and delivery to the proteasome for degradation, which prevents protein aggregation. Pathological variants of HTT compete with newly synthesized, misfolded proteins for access to a limited pool of enzymes and effectors of K11/K48-specific quality control.

Key Resources Table

REAGENT or RESOURCE	SOURCE	IDENTIFIER
Antibodies		
Anti-K11/48 bispecific polyubiquitin linkage-specific antibody	This paper	N/A
Anti-K11/gD bispecific control antibody	This paper	N/A
Anti-K48/gD bispecific control antibody	This paper	N/A
Anti-M1 polyubiquitin linkage-specific antibody	Genentech	Clone 1F11/3F5/Y102L
Anti-K11 polyubiquitin linkage-specific antibody	Genentech	Clone 2A3/2E6
Anti-K48 polyubiquitin linkage-specific antibody	Genentech	Clone Apu2.07
Anti-K63 polyubiquitin linkage-specific antibody	Genentech	Clone Apu3.A8
Anti-gD antibody	Genentech	Clone 5B6
Peroxidase conjugated AffiniPure F(ab')$_2$ goat anti-human IgG, Fcγ fragment specific secondary	Jackson ImmunoResearch	Cat#109-036-098
Anti-Ubiquitin antibody (P4D1)	Abcam	Cat#ab139101
Anti-Puromycin antibody	EMD Millipore	Cat#MABE343
Anti-HIS tag antibody	Abcam	Cat#ab18184
Anti-Bag6 antibody	Santa Cruz biotechnology, Cell Signaling Technology	Cat#sc-365928, Cat#8523S
Anti-p97 antibody	Abcam	Cat#ab11433
Anti-p62/SQSTM1 antibody	Abcam	Cat#ab56416
Anti-Ubiquilin 2 antibody	Novus	Cat#NBP1-85639
Anti-FLAG tag antibody	Sigma-Aldrich	Cat#F1804-1MG
Anti-HA tag antibody	Cell Signaling Technology	Cat#3724S
Anti-Ubr5 antibody	Bethyl Laboratories; Cell Signaling Technology	Cat#A300-573A; Cat#8755S
Anti-Ube2S antibody	Abcam	Cat#ab177508
Anti-Cyclin B1 antibody	Santa Cruz Biotechnology	Cat#sc-245
Anti-Securin antibody	Santa Cruz Biotechnology	Cat#sc-22772
Anti-Geminin antibody	Santa Cruz Biotechnology	Cat#sc-13015
Anti-Cyclin A antibody	Santa Cruz Biotechnology	Cat#sc-596
Anti-Nek2 antibody	BD Transduction Laboratories	Cat#610594
Anti-Cdc20 antibody	Santa Cruz Biotechnology	Cat#sc-13162
Anti-GFP antibody	Santa Cruz Biotechnology	Cat#sc-8334
Anti-GAPDH antibody	Cell Signaling Technology	Cat#2118S
Anti-Actin antibody	MPbio	Cat#691001
Anti-HSP90β antibody	Cell Signaling Technology	Cat#5087
Anti-Huntingtin antibody	EMD Millipore	Cat#EM48
Anti-HUWE1 antibody	Bethyl Laboratories	Cat#A300-486A
Anti-OCT4 antibody	Santa Cruz Biotechnology	Cat# ac-8628
Anti-Tuj1 antibody	Cell Signaling Technology	Cat#5568
Anti-Pax6 antibody	Biolegend	Cat# PRB-278B

REAGENT or RESOURCE	SOURCE	IDENTIFIER
Anti-NANOG antibody	Cell Signaling Technology	Cat#3580
Bacterial and Virus Strains		
E. coli BL21-DE3 competent cells	NEB	Cat#C2527I
E.coli: One Shot Stbl3 Chemicallly competent cells	Thermo Fisher	Cat#C737303
Chemicals, Peptides, and Recombinant Proteins		
cOmplete™, EDTA-free protease inhibitor cocktail tablets from Roche	Sigma-Aldrich	Cat#11873580001
Phenylmethanesulfonyl fluoride	Sigma-Aldrich	Cat#P7626
Methylated monoUb	Boston Biochem	Cat#U-501
UBE1	Boston Biochem	Cat#E-304
Uev1a/UbcH13	Boston Biochem	Cat#E2-664
Ubiquitin (monoUb)	Boston Biochem	Cat#U-100H
M1-linked diUb	Boston Biochem	Cat#UC-700B
K6-linked diUb	Boston Biochem	Cat#UC-11B
K11-linked diUb	Boston Biochem	Cat#UC-40B
K27-linked diUb	UBPBio	Cat#D5210
K29-linked diUb	Boston Biochem	Cat#UC-81B
K33-linked diUb	Boston Biochem	Cat#UC-101B
K48-linked diUb	Boston Biochem	Cat#UC-200B
K63-linked diUb	Boston Biochem	Cat#UC-300B
K6 monoUb	Boston Biochem	Cat#UM-K60
K11 monoUb	Boston Biochem	Cat# UM-K110
K27 monoUb	Boston Biochem	Cat# UM-K270
K29 monoUb	Boston Biochem	Cat# UM-K290
K33 monoUb	Boston Biochem	Cat# UM-K330
K48 monoUb	Boston Biochem	Cat# UM-K480
K63 monoUb	Boston Biochem	Cat# UM-K630
K11R monoUb	Boston Biochem	Cat# UM-K11R
K48R monoUb	Boston Biochem	Cat# UM-K48R
K11R K48R monoUb	Meyer & Rape, 2014	N/A
M1/K63 branched Ub trimers	This paper	N/A
K11/K48 branched Ub trimers	This paper	N/A
Reduced glutathione	Sigma-Aldrich	Cat#G4251
PNGase F	NEB	Cat#P0704L
Carboxypeptidase B from pig pancreas from Roche	Sigma-Aldrich	Cat#10103233001
Nocodazole	Sigma-Aldrich	Cat#M1404
Thymidine	Sigma-Aldrich	Cat#T9250-25G
Z-Leu-Leu-Leu-al (MG132)	Thermo Fisher Scientific	Cat#I13005M
Antimycin A	Sigma-Aldrich	Cat#A8674-25MG
Oligomycin	Thermo Fisher Scientific	Cat#ICN15178601

REAGENT or RESOURCE	SOURCE	IDENTIFIER
Pifithrin-μ	Sigma-Aldrich	Cat#P0122-5MG
VER-155008	Sigma-Aldrich	Cat#SML0271-5MG
17-DIMETHYLAMINOETHYLAMINO-17-DEMETHOXYG (17-DMAG)	Sigma-Aldrich	Cat#D5193-1MG
Dithiothreitol (DTT)	Invitrogen	Cat#15508-013
N^2,N^4-Dibenzylquinazolinine-2,4-diamine (DBeQ)	Sigma-Aldrich	Cat#SML0031-5MG
Carbonyl cyanide 3-chlorophenylhydrazone (CCCP)	Abcam	Cat#ab141229
Doxorubicin	Sigma-Aldrich	Cat# D1515-10MG
Chloroquine	Thermo Fisher Scientific	Cat#ICN19391910
Tunicamycin	Sigma-Aldrich	Cat#T7765-1MG
Homoharringtonine	LKT Laboratories	Cat#H0169
Emetine dihydrochloride hydrate	Sigma-Aldrich	Cat#E2375
α-Amanitin	Sigma-Aldrich	Cat#A2263
Dimethylsulfoxide	Thermo Fisher Scientific	Cat#BP231-100
Puromycin	Sigma-Aldrich	Cat#P8833-100
Cycloheximide	Sigma-Aldrich	Cat#C7698-5G
Hoechst 33342	AnaSpec Inc.	Cat#83218
S-Trityl-L-cysteine (STLC)	Sigma-Aldrich	Cat#16739-5G
N-Ethylmaleimide	Sigma-Aldrich	Cat#E3876
Critical Commercial Assays		
QuikChange Lightning Site-Directed Mutagenesis Kit	Agilent	Cat#210518
Alexa Fluor® 488 Protein Labeling Kit	Thermo Fisher Scientific	Cat#A10235
Alexa Fluor® 546 Protein Labeling Kit	Thermo Fisher Scientific	Cat#A10237
Experimental Models: Cell Lines		
Hamster: CHO cells	Genentech	N/A
Human: HeLa cells	ATCC	N/A
Human: HEK293T cells	ATCC	N/A
Human: Passage 42 H1 ES cells	WiCell Research Institute	N/A
Human: FLAG-UBR4 HEK293T cells	This paper	N/A
Human: FLAG-UBR5 HEK293T cells	This paper	N/A
Experimental Models: Organisms/Strains		
Mouse: 175Q HD Knock-in	Menalled et al., 2012	N/A
Oligonucleotides		
K63R ubiquitin primer forward: CCCTGTCAGACTATAATATCCAAAGAGAATCGACGCTG	This paper	N/A
K63R ubiquitin primer reverse: CAGCGTCGATTCTCTTTGGATATTATAGTCTGACAGGG	This paper	N/A
siRNA targeting sequence: Bag6 #1: GAGGAGGATCAGCGGTTGA	GE Dharmacon	Cat#L-005062-01
siRNA targeting sequence: Bag6 #2: TGTTATCAATGGCCGAATT	GE Dharmacon	Cat#L-005062-01
siRNA targeting sequence: Bag6 #3: TCTCTATGGTGGACGTAGT	GE Dharmacon	Cat#L-005062-01
siRNA targeting sequence: Bag6 #4: ACATTCAGAGCCAGCGGAA	GE Dharmacon	Cat#L-005062-01

REAGENT or RESOURCE	SOURCE	IDENTIFIER
siRNA targeting sequence: Ubr5 #1: GCACTTATATACTGGATTA	GE Dharmacon	Cat#L-007189-00, Cat#J-007189-06
siRNA targeting sequence: Ubr5 #2: GATTGTAGGTTACTTAGAA	GE Dharmacon	Cat#L-007189-00, Cat#J-007189-07
siRNA targeting sequence: Ubr5 #3: GATCAATCCTAACTGAATT	GE Dharmacon	Cat#L-007189-00, Cat#J-007189-08
siRNA targeting sequence: Ubr5 #4: GGTCGAAGATGTGCTACTA	GE Dharmacon	Cat#L-007189-00, Cat#J-007189-09
siRNA targeting sequence: Ubr4 #1: GGGAACACCCTGACGTAAA	GE Dharmacon	Cat#L-014021-01, Cat#J-014021-09
siRNA targeting sequence: Ubr4 #2: TCATGAAGCCTGTTCGAAA	GE Dharmacon	Cat#L-014021-01, Cat#J-014021-10
siRNA targeting sequence: Ubr4 #3: CTACGAAGCTGCCGACAAA	GE Dharmacon	Cat#L-014021-01, Cat#J-014021-11
siRNA targeting sequence: Ubr4 #4: TGAACAAATTTGCCGATAA	GE Dharmacon	Cat#L-014021-01, Cat#J-014021-12
siRNA targeting sequence: Ube2S: GGCACUGGGACCUGGAUUU	Kelly et al., 2014	N/A
Forward primer for UBR5 sgRNA: CACCGcacgaaatggatggacgtca	This paper	N/A
Reverse primer for UBR5 sgRNA: AAACtgacgtccatccatttcgtgC	This paper	N/A
Donor oligo DNA for FLAG tag insertion at the N-terminus of UBR5: gggctgggggcgggcgagagcgggaggggccgccctcgagt ggaggacgagaaggaaagcaccatgGACTACAAGGACC ACGACGGTGACTACAAGGACCACGACATCGAC TACAAGGACGACGACGACAAGacgtccatccatttcgt ggttcacccgctgccgggcaccgaggaccagctcaatgacaggta atag	This paper	N/A
Forward primer for UBR4 sgRNA: CACCGcggaagatggcgacgagcgg	This paper	N/A
Reverse primer for UBR4 sgRNA: AAACccgctcgtcgccatcttccgC	This paper	N/A
Donor oligo DNA for FLAG tag insertion at the N- terminus of UBR4: ctcctgggaggcggcgctgggccggtggcaagccccccggaggga gccgcagtagtacgacggaagatgGACTACAAGGACCA CGACGGTGACTACAAGGACCACGACATCGACT ACAAGGACGACGACGACAAGgcgacgagcggcggc gaagaggcggcggcagcggctccggcgccggggaccccggca acgggggcg	This paper	N/A
Recombinant DNA		
pET-15b di-UbLinear	Genentech	N/A
pRK hIgG1 knob half antibody expression vector	Genentech	N/A
pRK hIgG1 hole half antibody expression vector	Genentech	N/A
pInducer20 HTT-73Q-GFP	This paper	N/A
pInducer20 HTT-23Q-GFP	This paper	N/A
pCS2 6xHIS-HTT-73Q	This paper	N/A
pCS2 6xHIS-HTT-23Q	This paper	N/A
pLenti 3xFLAG -USP5	This paper	N/A
pLenti 3xFLAG -CUED2	This paper	N/A
pLenti 3xFLAG -UBXD2	This paper	N/A
pCS2 HA-p47	This paper	N/A
pCS2 HA-FAF1	This paper	N/A
pCS2 HA-FAF2	This paper	N/A
pCS2 HA-SAKS1	This paper	N/A
pCS2 HA-UBXD7	This paper	N/A
pCS2 HA-RPN10	This paper	N/A
pCS2 HA-HHR23A	This paper	N/A
pX330-sgRNA_UBR5	This paper	N/A

REAGENT or RESOURCE	SOURCE	IDENTIFIER
pX330-sgRNA_UBR4	This paper	N/A
pMAL-p97	Meyer & Rape, 2014	N/A
pET28-p47	Meyer & Rape, 2014	N/A
pCS2 HIS-ubiquitin64TEV/FLAG	Meyer and Rape, 2014	N/A
pCS2 ubiquitin64TEV/FLAG	This paper	N/A
Software and Algorithms		
ImageJ	NIH	https://imagej.nih.gov/ij/
Biaevaluation 4.1	GE Healthcare	
Other		
Ni-NTA agarose	Qiagen	Cat#30210
Amylose Resin	NEB	Cat#E8021L
HiLoad 26/600 Superdex 75 column	GE Healthcare	Cat#28989334
Mono-S 5/50 GL column	GE Healthcare	Cat#17516801
MabSelect SuRe resin	GE Healthcare	Cat#17543801
Dionex ProPac HIC-10 column (5 μm, 7.8×75 mm)	Thermo Fisher Scientific	Cat#063665
XBridge Protein BEH 200 Å column (3.5 μm, 7.8×300 mm)	Waters	Cat#176003596
Reverse-phase chromatography PLRP-S 300 Å column (3 μm, 4.6×50 mm)	Agilent	Cat#PL1512-1301
TransIT-293 Transfection Reagent	Mirus	Cat#MIR2705
Bolt® 4–12% Bis-Tris Plus gels	Thermo Fisher Scientific	Cat#NW04120BO X
20X Bolt® MES SDS running buffer	Thermo Fisher Scientific	Cat#B0002
Nitrocellulose membrane, 0.2 μm	Thermo Fisher Scientific	Cat#88024
SuperSignal West Pico chemiluminescent substrate	Thermo Fisher Scientific	Cat#34077
Protein G-Agarose beads	Roche	Cat#11719416001
ANTI-FLAG M2 Affinity Gel	Sigma-Aldrich	Cat#A2220
3X FLAG Peptide	Sigma-Aldrich	Cat#F4799
mTeSR1	StemCell Technologies Inc.	Cat#05871/05852
STEMdiff Neural induction medium	StemCell Technologies Inc.	Cat#05831
Collagenase	StemCell Technologies Inc.	Cat#07909
Accutase	StemCell Technologies Inc.	Cat#07920
Biacore sensor CM5 chip	GE Healthcare	BR100012
Biacore amine-coupling kit	GE Healthcare	BR100050